

**Key Points:**

- Bottom water temperature at Jordan Basins is warmer during winter than summer, which is distinctly different from neighboring shelf seas
- This unique seasonality reflects a delayed response (approximately 3 months) of Jordan Basin to the changes in the slope sea
- Deep water at Jordan Basin is affected by the Nova Scotia Current and Gulf Stream warm-core rings

**Correspondence to:**



J. Du,  
[jdu@whoi.edu](mailto:jdu@whoi.edu);  
[jiabi.du@gmail.com](mailto:jiabi.du@gmail.com)

**Citation:**

Du, J., Zhang, W. G., & Li, Y. (2021). Variability of deep water in Jordan Basin of the Gulf of Maine: Influence of Gulf Stream warm core rings and the Nova Scotia Current. *Journal of Geophysical Research: Oceans*, 126, e2020JC017136. <https://doi.org/10.1029/2020JC017136>

Received 27 DEC 2020  
 Accepted 1 MAY 2021

## Variability of Deep Water in Jordan Basin of the Gulf of Maine: Influence of Gulf Stream Warm Core Rings and the Nova Scotia Current

Jiabi Du<sup>1</sup> , Weifeng G. Zhang<sup>1</sup> , and Yizhen Li<sup>2</sup>

<sup>1</sup>Applied Ocean Physics and Engineering Department, Woods Hole Oceanographic Institution, Woods Hole, MA, USA,

<sup>2</sup>CSS Inc. under contract to NOAA National Centers for Coastal Ocean Science, Silver Spring, MD, USA

**Abstract** As the nutrient-rich subsurface slope water intruding into the deep basin of the Gulf of Maine (GoM) supports the high biological productivity in the semi-enclosed gulf, it is important to understand the process and time scale of such slope water intrusion. This study focuses on variations of the GoM deep water on seasonal to interannual time scales and the influences of open ocean processes on the temporal variation of the deep water properties. Based on long-term monitoring data, it is found that the deep water at Jordan Basin (one of three major basins in the GoM) is persistently warmer in winter than in summer, which is distinctly different from the seasonality of surface water in the basin and the deep water on neighboring shelf seas. The unique seasonality in the deep GoM reflects a time-lagged response to shoreward intrusion of the subsurface slope water off the GoM. Both observation-based lag-correlation analyses and numerical simulations confirm a timescale of approximately 3 months for the intruding subsurface slope water to flow from Northeast Channel to Jordan Basin. Properties of the intruding slope water at the Northeast Channel were significantly correlated with the Gulf Stream position and dramatically impacted by episodic warm-core rings shed from Gulf Stream. Inside the deep GoM, the intruding slope water was also indirectly affected by the fresher water input from Nova Scotia Current. Spreading of the fresher water inside the gulf strengthens near-surface stratification, suppresses deep convection, and preserves heat and salt in the deep GoM during the wintertime.

**Plain Language Summary** Nutrient-rich slope water intruding into the deep basin of the Gulf of Maine provides 30% of the nutrients needed to support the high biological productivity and high yield fisheries in the gulf. Our analysis of long-term mooring data shows that the deep water in the Gulf of Maine changes in a unique fashion: being warmer in winter and colder in summer. This unique seasonality differs dramatically from the deep water on the neighboring continental shelves. It represents a delayed response of the deep water in the gulf to seasonal changes of the major currents in the adjacent open ocean. We explained the timescale of this delayed response from multiple angles using mooring data, numerical simulations, and remote sensing data. We found that signal of open ocean change at shelf edge (e.g., induced by Gulf Stream meandering and associated eddies) propagates into the deep gulf basin in about 3 months. Meanwhile, the surface buoyant and low-salinity inflow from the upstream Scotian Shelf into the Gulf of Maine tends to suppress vertical mixing in the gulf and helps maintain the heat and salt stored in the deep gulf even in the wintertime when the surface ocean loses heat to the cold atmosphere.

### 1. Introduction

The exchange between shelf seas and deep oceans, a central question in coastal physical oceanography (Brink, 2016), regulates how nutrients, biota, and other materials are delivered to or removed from the coastal regions. It is particularly important for the semi-enclosed Gulf of Maine (GoM), one of the most important fishing ground in the US (Pershing et al., 2015), since a major source of the nutrients to sustain the high biological productivity in GoM comes from the subsurface water on the neighboring continental slope (hereafter referred to as *slope water*) that intrudes into the deep GoM (Townsend et al., 1998, 2010). The intruding slope water supplies approximately 30% of the nutrients needed for the primary biological production in the GoM (Schlitz & Cohen, 1984). The slope water condition and the intrusion is subject to the influence of large-scale climate variations. For instance, recent studies (Smith & Pettigrew, 2012; Townsend et al., 2010, 2015) identified changing nutrient conditions in GoM with less nutrient input from

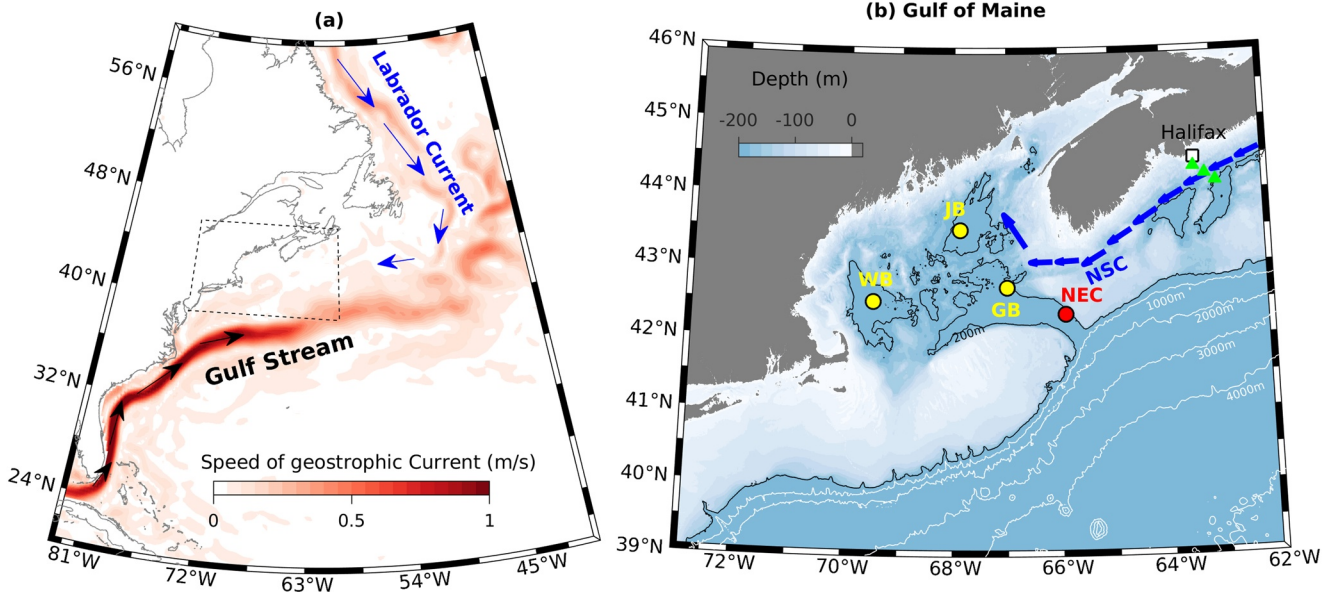


**Figure 1.** Regional map of the (a) northwest Atlantic Ocean and (b) Gulf of Maine. The filled color in (a) indicates the speed of surface geostrophic current calculated based on the mean sea surface height of 1993–2018. In (b), three major basins with depth exceeding 200 m are marked with yellow dots (GB for Georges Basin; JB for Jordan Basin; WB for Wilkinson Basin). Also marked are Northeast Channel (NEC, red dot), Nova Scotia Current (NSC, blue arrows), and three ADCPs (green triangles) deployed to measure the NSC.

the slope water because accelerated Arctic melting strengthens the Nova Scotia Current that feeds into the surface layer of the GoM.

GoM is a semi-enclosed shelf sea in the Northwest Atlantic Ocean. While the GoM surface water is openly connected with the Atlantic Ocean, its deeper part, below 100 m, is highly topographically confined and only connected with the Atlantic Ocean through the Northeast Channel (NEC), which is 35 km wide, approximately 230 m deep, and oriented northwest-southeast (Figure 1b). The deep part of GoM is mainly comprised of three basins with maximum depth greater than 200 m, namely the Georges Basin, Jordan Basin, and Wilkinson Basin. Among them, Jordan and Wilkinson Basin is deeper, with maximum depth exceeding 250 m. The deep basins of the GoM are filled with salty, warm water. This deep water of the GoM mainly originates from two slope water masses (1) *Warm Slope Water* of mostly Gulf Stream origin and (2) *Labrador Slope Water* of mostly Labrador Current origin. The former is warmer and saltier, contains more nutrients (Townsend et al., 2015), and dominates the top 300 m of the slope sea off the NEC (Houghton & Fairbanks, 2001).

The bottom water in the GoM is separated from the surface by a thermocline layer at 50–120 m below the surface (Figure 2). The depth and temperature gradient of the thermocline layer vary seasonally. During summer, temperature in the thermocline layer decreases with increasing depth, while the opposite trend occurs in winter. There is also occasional temperature minimum in the thermocline layer, which indicates the formation of the intermediate thermocline water from vertical mixing of the surface and deep waters in the gulf (Hopkins & Garfield, 1979). The deep water property is mostly affected by the intrusion of the slope waters, but local processes, such as river discharge, lateral exchange with shallower coastal waters, and tidal mixing, also play a role. Another local process that could dramatically affect the bottom water property in the GoM is the wintertime convection, which occurs in some of the winters, and its strength is highly dependent on the surface salinity during the winter (Brown & Beardsley, 1978).

GoM has experienced substantial changes in recent decades. Induced by changes in both local atmospheric conditions and open ocean dynamics, such as a northward shift of the Gulf Stream (Rossby & Benway, 2000), water in the GoM warmed up rapidly in 2004–2013 and the associated warming rate exceeded more than 98% of the global ocean over the same period (Pershing et al., 2015). The relative contributions of the local processes (e.g., surface heat flux) versus the remote influences (e.g., intrusion of the warm slope

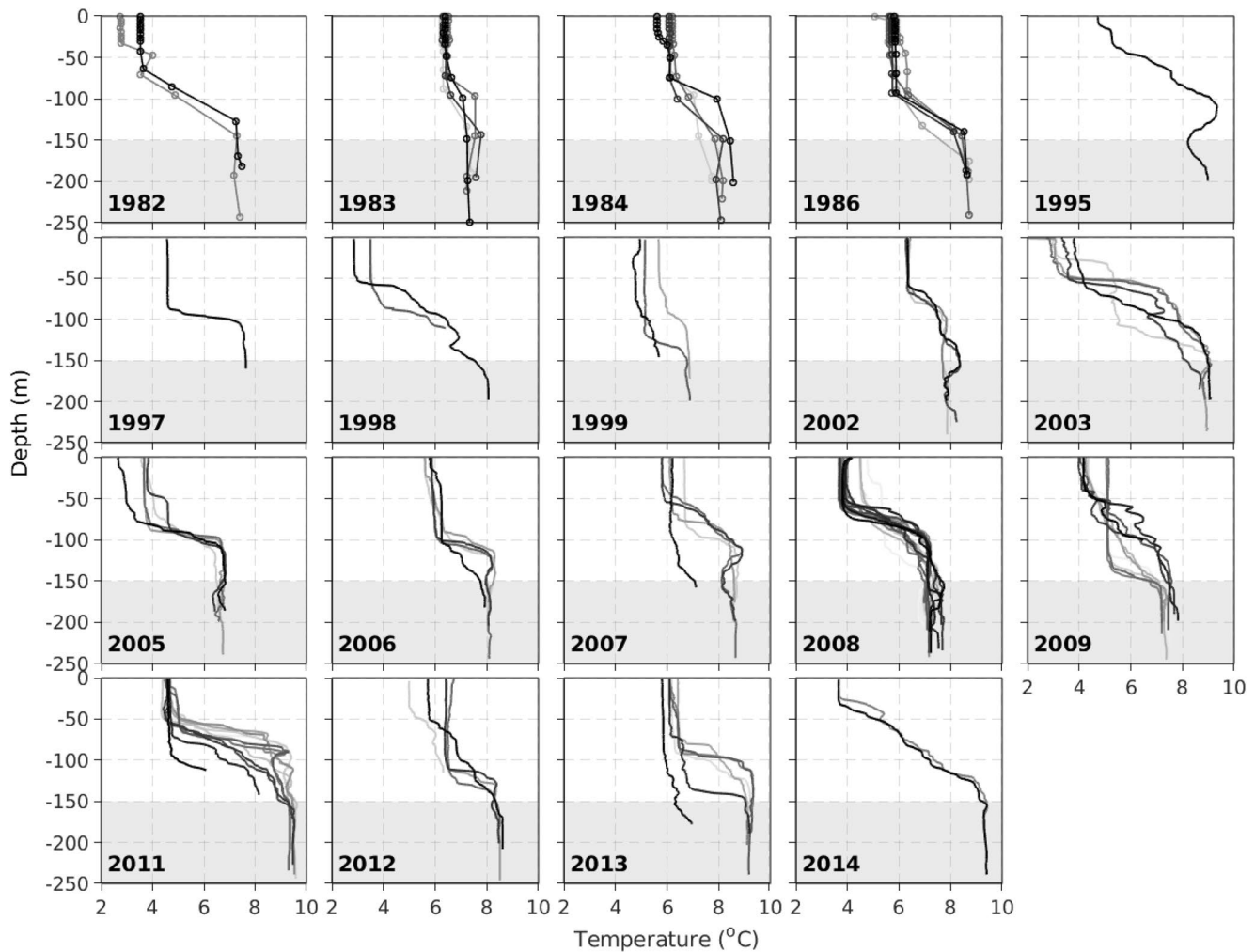


**Figure 2.** January-March in situ temperature profiles in a region within 50 km from the basin station (43.49°N, 67.88°W) in the period of 1978–2014 extracted from the NOAA historical hydrographic survey dataset. These wintertime temperature profiles suggest the water column in Jordan basin is stratified with a well-mixed bottom layer below 150 m (highlighted by the gray patches).

water) to the warming in the GoM is unknown. Since water in the deep GoM is largely affected by the intruded slope water (Smith et al., 2001), conditions of the deep water in the gulf can be used to indicate the remote influence from the open ocean. Advances in understanding the deep gulf water variability will thus help to answer the question related to the local versus remote influences.

Slope water intrusion in GoM has long been studied. Ramp et al. (1985) estimated that the average inflow of the slope water through the NEC is  $0.26 \pm 0.06$  Sv ( $1 \text{ Sv} = 10^6 \text{ m}^3 \text{ s}^{-1}$ ). Upon entering the GoM, the intruding slope water is carried into the gulf interior by a large-scale cyclonic flow in the gulf basin (Bigelow, 1927; Xue et al., 2000). Mountain and Jessen (1987) revealed a clear temperature-salinity signal progression following the cyclonic flow along the edge of the deep gulf, and suggested approximately equal contributions of advection and mixing in determining the deep gulf water properties. These studies, however, did not depict a clear picture of the temporal variations of the deep gulf conditions. Several questions remain unanswered, such as how the slope water off GoM is affected by open ocean dynamics, how long it takes for changes at the slope sea to impact the inner gulf, and what will impact the intruding water after it was transported into the deep GoM.

Here, we analyzed the seasonal and interannual variability of the GoM deep water, based on long-term historical measurements at two mooring stations, one at the NEC representing the shelf edge condition and the other at Jordan Basin representing the inner gulf. We found a unique seasonality of the deep water in

Jordan Basin: consistently *higher* temperature in winter than in summer. This unusual seasonal variation is opposite to that of the basin surface water and causes a vertically out-of-phase seasonality at the basin station, which is in contrast to the more synchronized water-column temperature variation at the NEC. We explain the unusual seasonal temperature variation of the deep basin water by synthesizing *in situ* and remote sensing data including sea-surface height and sea-surface temperature, along with a numerical model. The analysis here establishes a statistical connection of the bottom water in inner gulf with open ocean processes, including the Gulf Stream, associated warm-core rings, and the Nova Scotia Current. The dynamical mechanism of the connection is left for future studies.

## 2. Methods

### 2.1. In Situ Measurements

Observational data at two moorings stations, one in the NEC and the other in Jordan Basin (see Figure 1b for their locations), were analyzed to examine the seasonal and interannual variability of bottom water in the inner gulf and intruding slope water at the shelf edge. Both moorings are part of the University of Maine Ocean Observing System, which is a component of the Northeastern Regional Association of Coastal Ocean Observing Systems (<http://www.neracoos.org>). At the Jordan Basin station (hereafter referred to as the *basin station*), seven Seabird SE27 conductivity-temperature-depth (CTD) sensors were deployed at different depths (1, 20, 50, 100, 150, 200, and 250 m below surface). Also available is a downward-looking acoustic-Doppler current profiler (ADCP) measuring the horizontal water velocity at 8-m vertical resolution. At the NEC station (hereafter referred to as the *channel station*), a similar vertical configuration of instruments was used, but with six CTD sensors at 1, 20, 50, 100, 150, and 180 m below surface, respectively. Note that the measurements at the NEC station do not necessarily represent the condition of the entire channel. The current in the NEC is characterized with a northwestward inflow at the eastern side of the channel and a southeastward outflow at the western side, and this pattern of laterally sheared flow persists over the water column (Smith et al., 2012). The channel station measurements capture the intrusion flow on the northeast half of the channel and can be used to examine the variations of intruding slope water. Details of the buoys are given in Pettigrew et al. (2011).

Hourly data from July 09, 2003 (March 06, 2004) to the present are available with minor data gaps at the basin (channel) station. The data gaps are caused by malfunctions or maintenance of the instruments, and occupy 13% and 7% of the time in CTDs and 19% and 11% in ADCPs at the basin and channel stations, respectively. Time-series data of temperature, salinity, and velocity were low-pass filtered in this study with a cutoff frequency of  $1/50 \text{ h}^{-1}$  to remove the tidal and diurnal fluctuations. The climatological seasonality and anomalies of temperature, salinity, potential density, and velocity were extracted based on the low-pass filtered results. The seasonal climatology was obtained by averaging the corresponding monthly mean values over the available years, and the anomalies here refer to the difference between the low-pass filtered values and the seasonal climatology.

To examine the temperature variation in the deep basin over a longer historical period, we analyzed a 42-year (1977–2018) hydrographic data set collected by the NOAA Northeast Fisheries Science Center. Hydrographic data in waters off the Northeast U.S. coast including Mid-Atlantic Bight, Southern New England, Georges Bank, and Gulf of Maine were collected six times a year since the 1970s (<https://www.fisheries.noaa.gov/feature-story/monitoring-northeast-shelf-ecosystem>). We used the ship-survey temperature data within the GoM only. The survey temperature before 1987 were measured with bottles, while that after 1988 were measured with Sea-Bird CTDs.

Along-shelf velocity measured by upward-looking ADCPs on the Scotian Shelf is analyzed to investigate the potential influence of the Nova Scotia Current on the deep water at Jordan Basin. Continuous velocity measurements are available at three sites across the inner Scotian Shelf at Halifax, Canada for the 10-year period of 2008–2018 (Dever et al., 2016; Hebert, Pettipas, & Brickman, 2020). The three sites are approximately 40 km apart (see Figure 1b for their locations). As revealed by *in situ* glider measurements and calculated geostrophic current (Dever et al., 2016), the middle site, which is 40 km off the coast, is close to the maxima of the alongshore velocity, and the other two sites are located near the edges of the Nova Scotia Current. The velocity profiles from all the three sites are integrated in both vertical and cross-shelf



directions to obtain the along-shelf transport of the Nova Scotia Current. Note that the relatively low cross-shelf resolution of the velocity measurements might cause errors in the absolute values of the estimated along-shelf transport. But the depth and cross-shore integrated flux likely captures the temporal variability the along-shelf transport, which is the part that is mostly relevant to this study. In particular, anomalies of the Nova Scotia Current transport relative to the 10-years seasonal mean is used in the analysis here.

## 2.2. Detection of Gulf Stream and Warm-Core Rings

The Gulf Stream downstream of the Cape Hatteras is unstable and often develops large-amplitude meandering waves (Andres, 2016; Cornillon, 1986; Halliwell & Mooers, 1983), which could then detach from the Gulf Stream and form mesoscale eddies, so-called cold-core or warm-core rings (e.g., Chaudhuri et al., 2009; Csanady, 1979; Gangopadhyay et al., 2019). Warm-core rings carry warm and salty Gulf Stream water and tend to move westward along the shelf edge due to planetary and/or topographic beta effects (Lai & Richardson, 1977). During their westward migration, they interact with the slope and shelf waters (e.g., Bisagni & Smith, 1998). Impinging warm-core rings have been found to induce substantial water exchange across the shelf edge at the neighboring Mid-Atlantic Bight (e.g., Joyce et al., 1992; Zhang & Partida, 2018), including direct intrusion of the ring water onto the shelf (Zhang & Gawarkiewicz, 2015).

To understand the impact of the Gulf Stream and warm-core rings on the water conditions in the slope sea adjacent to the GoM, we extracted the track of the Gulf Stream in the northwest Atlantic Ocean based on sea surface height (SSH) measured by satellite altimeters. The gridded global SSH data in 1993–2018 from European Union Copernicus Marine Environmental Monitoring Service (<https://marine.copernicus.eu>) were used here (Mertz & Legeais, 2020). The data have a horizontal resolution of  $0.25^\circ$  and daily temporal resolution, high enough to capture the Gulf Stream and warm-core rings. The Gulf Stream track is identified with the 25 cm SSH contour, following previous studies (Andres, 2016; Lillibridge & Mariano, 2013; Rossby et al., 2014). An auto-detection scheme for anticyclonic warm-core rings was applied, following the method of Isern-Fontanet et al. (2003). The rings are identified based on the Okubo-Weiss parameter ( $W$ ), which measures the relative importance of deformation and rotation. It is calculated as the sum of the squares of the normal and shear components of strain minus the square of the relative vorticity. For a nondivergent horizontal flow in the ocean, it is

$$W = 4 \left( \left( \frac{\partial u}{\partial x} \right)^2 + \frac{\partial u}{\partial y} \frac{\partial v}{\partial x} \right)$$

where the eastward and northward geostrophic velocity components were computed from the altimeter SSH as  $u = \frac{-g}{f} \frac{\partial h}{\partial y}$  and  $v = \frac{g}{f} \frac{\partial h}{\partial x}$ , respectively. Here,  $h$  is the SSH,  $g$  is the gravitational acceleration, and  $f$  is the Coriolis parameter. Closed contours of  $W = -2 \times 10^{-12} \text{ s}^{-2}$  were used in this study to identify the rings, following a previous study on the analysis of mesoscale eddies in the global ocean (Chelton et al., 2007). Two types of rings were detected based on the Okubo-Weiss number: anticyclonic warm core rings and cyclonic cold core rings. Rings with an SSH maximum at the centers were regarded as warm-core rings. Because of the low spatial resolution (approximately 20 km) of the SSH data, the auto-detection method here identifies only warm-core rings with diameters close to or larger than 100 km, and neglects smaller rings or eddies. Note that satellite sea surface temperature (SST) imagery is often used to identify individual warm-core rings (e.g., Zhang & Partida, 2018) or to manually draw ocean charts, which is then used to quantify the rings in the region (e.g., Gangopadhyay et al., 2019, 2020). However, the frequent cloud cover and dramatic seasonal variation in SST impose a great challenge to the application of automatic ring-detection algorithms.

## 2.3. Numerical Model

One major question to be answered in this study is the timescale of water mass moving from the shelf edge (i.e., at the NEC) to the inner gulf. In addition to the lag-correlation analysis based on observational data, we used a previously validated numerical model to determine the transport timescale by tracking the movement of released passive particles.

The computational GoM model used here is based on the Regional Ocean Modeling System (ROMS), which is a free-surface, hydrostatic, primitive-equation model with a terrain-following vertical coordinate (Shchepetkin & McWilliams, 2005). The GoM model has been validated and used in previous studies to examine the GoM circulation (He et al., 2008; Li et al., 2009, 2014). It has a horizontal resolution of 3 and 2 km in the along- and cross-shelf directions, respectively, and 36 vertical levels that are more closely spaced near the surface and bottom to better resolve boundary layers. Temperature, salinity, and velocity on the open lateral boundaries were extracted from the global data-assimilative Hybrid Coordinate Ocean Model (HYCOM, <https://www.hycom.org/dataserver>) solutions. Flather and Chapman open boundary conditions with external values obtained from the HYCOM solutions were used for free surface and depth-averaged velocity. Tidal harmonics in sea level and depth-averaged velocity of M2, S2, N2, K2, K1, O1, and Q1 frequencies extracted from an ADCIRC simulation of the western Atlantic (<http://adcirc.org/products/adcirc-tidal-databases>) were imposed on the model open boundaries. The Mellor-Yamada 2.5 closure scheme was used to parameterize the vertical turbulent mixing, and the quadratic bottom drag with a drag coefficient of 0.003 was applied. More detailed descriptions of the model are provided in previous work (He et al., 2008; Li et al., 2009, 2014).

Surface atmospheric forcing, including cloud fraction, precipitation, surface pressure and humidity, air temperature, surface wind, and shortwave radiation were extracted from the National Center for Environmental Prediction North America Regional Reanalysis product (Mesinger et al., 2006). Spatial and temporal resolutions of these forcing fields are approximately 32 km and 3 h, respectively. They were applied in the bulk flux formulation (Fairall et al., 2003) to derive wind stress and net surface heat and freshwater fluxes. Freshwater inputs from several major rivers along the GoM coastline were prescribed based on observed daily river runoff data from the U.S. Geological Survey. Hindcast simulations over a 10-year period of 2007–2016 were conducted.

Ten Lagrangian passive particles were released over a  $5 \times 5$  km region in the Northeast Channel at 100 m below the surface every 4 h of the 10-years simulation. The center of the release region is at the channel station. Within each year, about 22,000 particles are released. Their three-dimensional positions at each time were computed along with the other hydrodynamic variables, and the time of each particle first reaching the center of Jordan Basin, a  $0.4^\circ \times 0.4^\circ$  rectangular area around the basin station, was recorded. Over the 10-year simulation, approximately 10% of particles reach the center of Jordan Basin. The rest of the particles move into the shallow part of Jordan Basin, Georges Basin, or the slope sea due to the random nature of particle movement and the impact of tidal currents. To understand the connectivity between Jordan Basin and the NEC, we calculated the probability of the particles reaching each sub-region in the model domain. Following Feng and Hodges (2020), the probability function for a sub-region  $A$  over a period after release  $T$  is defined as

$$P(T, A) = \frac{1}{N_p T} \sum_{n=1}^{N_p} \int I_A(X_n(t)) dt$$

where  $X_n$  is the  $n$ th particle location,  $N_p$  is the number of released particles,  $t$  is time, and the subset indicator function  $I_A$  is

$$I_A(X_n) = \begin{cases} 1, & (X_n \in A) \\ 0, & (X_n \notin A) \end{cases}$$

For this study, we calculated the probability of 120 days after release for each subregion of  $0.1 \times 0.1^\circ$  in the entire model domain. Here,  $T = 120$  days is long enough for examining the connection between the NEC and Jordan Basin (see below).

### 3. Results

#### 3.1. Seasonality of GoM Deep Water

The long-term mooring data show decreasing temporal variability of temperature and salinity toward the bottom at both the basin and channel stations (Figure 3). Temperature and salinity at the basin station have

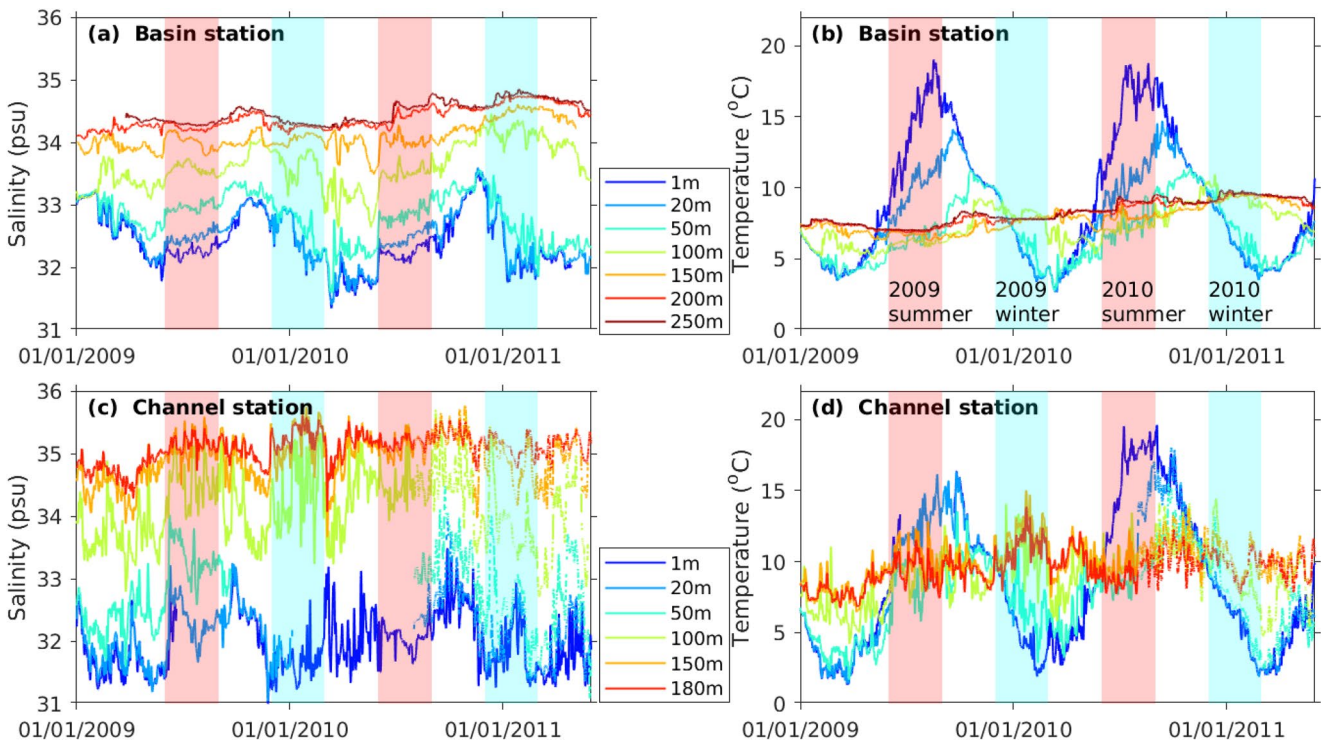


**Figure 3.** Time series of measurement salinity and temperature at different depths at the (a–b) basin and (c–d) channel stations over 2009–2011, as examples of the 16 years (2003–2018) long-term mooring data set. Red and cyan shades highlight the summer and winter periods. *Note* that the winter for a given year is from December of that year to February of the next year.

weak vertical variability for water below 150 m, and those at the channel station vary relatively little vertically for water below 100 m. The reduced vertical variation in temperature at the deep basin is also shown in the longer-term ship survey data (Figure 2). We hereby used the basin temperature and salinity at 150 m to represent properties of the deep basin water. Meanwhile, temperature and salinity at 100 m at the channel station were used in this study to establish the connection between the deep basin and deep channel waters, because they have similar mean potential density. Using temperature and salinity at 150 m at the channel station or the vertical mean temperature and salinity in the bottom layer gives a similar statistical result (not shown).

The seasonal mean vertical profiles of temperature and salinity averaged over the data-available years show distinctly different seasonal variability between the surface (0–50 m) and deep (below 150 m) layers at the basin station (Figures 4a–4d). At the surface, salinity reaches its maximum in November and minimum in June, and temperature reaches its maximum in August and minimum in March. These surface variations result presumably from seasonal changes in (i) the freshwater and heat input from coastal rivers and the Nova Scotia Current (Chapman & Beardsley, 1989; Smith, 1983) and (ii) the air-sea exchange of water and heat (Mountain & Manning, 1994). The deep layer at the basin station has much smaller seasonal variations of temperature and salinity, and the phases of the variations are nearly *opposite* to the seasonal signal in the surface layer (Figures 4a and 4b): Both temperature and salinity at the 150 m at the basin station are higher in winter (from December to February of the next year) and lower in summer (June–August) (Figures 4c and 4d). The T-S diagram indicates that properties of the deep basin water are more similar to the slope waters than the surface Scotian shelf water (Figure 5), which is consistent with the notion that the deep water in Jordan Basin originates from the slope sea.

At the channel station, seasonal variation of both temperature and salinity are relatively synchronized over the water column (Figures 4e and 4f). Temperature at 100 m maintains a high value in August–December, while the surface temperature reaches its maximum in August; Salinity at 100 m reaches the maximum in August, a month earlier than the surface salinity. Variabilities of the properties of the channel water at

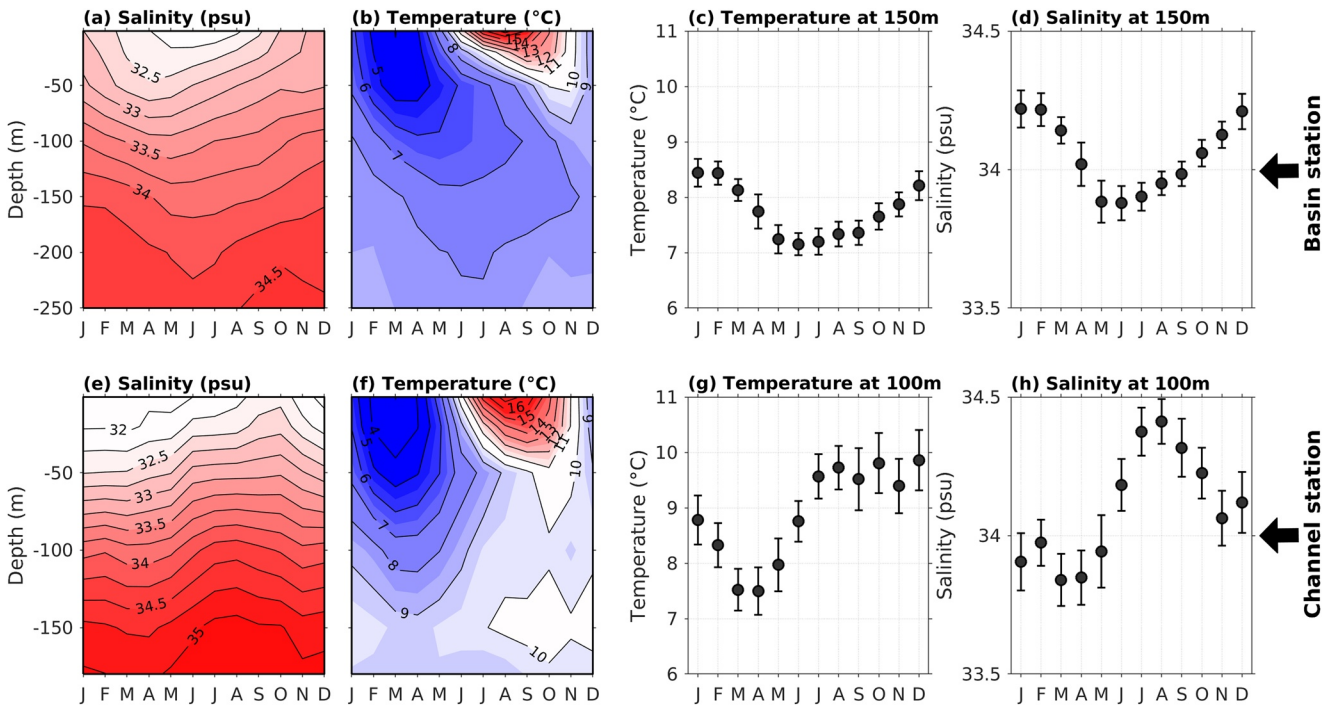


**Figure 4.** Climatological vertical profiles of salinity, temperature, and subsurface temperature at the basin station (a–d) and the channel station (e–h). The vertical bars in (c–d) and (g–h) represent the standard error of monthly mean.

100 m are much higher than those of the basin water at 150 m (Figure 3), consistent with the wider spread of the deep channel water in the T-S diagram (Figure 5). Similar to the deep water in the basin, the deep water in the channel also has properties very similar to the slope waters. Note that water at 150 m in the

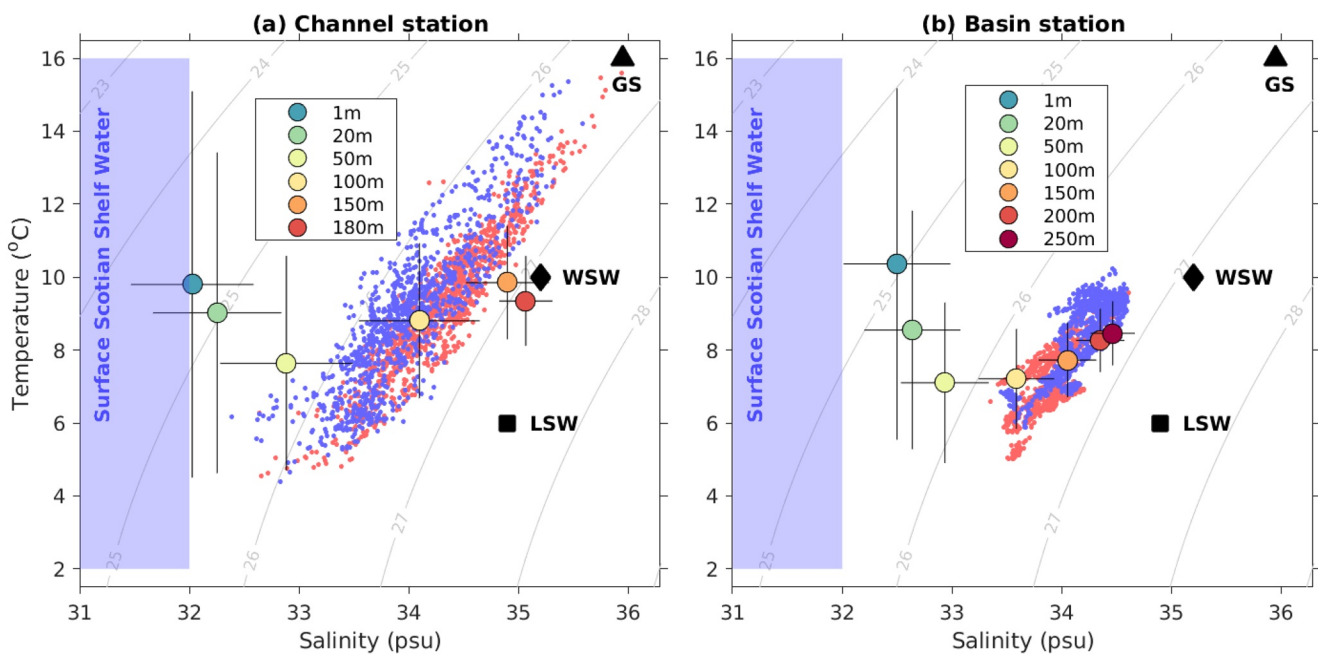


**Figure 5.** T-S diagram of data at different depths at the two stations. Small red and blue dots represent all the summer and winter data at (a) 100 m at the channel station and (b) 150 m at the basin station, respectively. The color-filled circles depict the mean T-S properties of water at different depths (see the legends), and the error bars of each filled circle denote one standard deviation. Black solid triangle, diamond, and square are nominal end-members for Gulf Stream Water (GS), Warm Slope Water (WSW), and Labrador Slope Water (LSW), following Houghton and Fairbanks (2001).



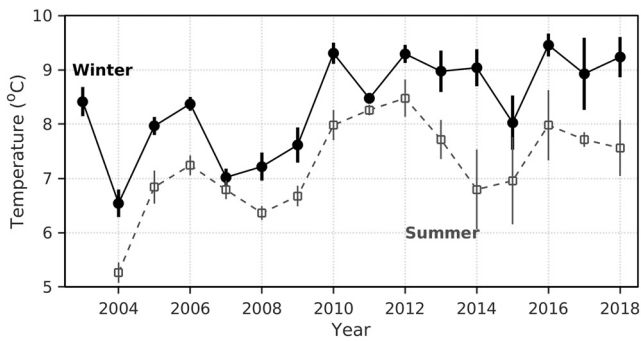


**Figure 6.** Interannual variability of summer (gray square) and winter (black dot) mean temperature at 150 m at the basin station. The vertical bars represent one standard deviation over the three months period, June-August for summer, and December-February for winter.

channel (the light orange circle in Figure 5a) has properties even closer to the slope waters, particularly to the warm slope water. Also noticeable from the T-S diagram is the wide spread of T-S properties of the deep water at the channel. Salinity at 100 m at the channel is 33.5–34.5 PSU, smaller than salinity of the two slope water masses. This lower salinity likely results from downward entrainment of the surface fresher water. Occasionally, the T-S characteristic of bottom water at the channel can be close to the Gulf Stream end member (with salinity approximately 36 PSU) in both summer and winter seasons. It suggests that the Gulf Stream water may exert direct influence on the slope sea condition near NEC, which will be furthered discussed in the next section.

The seasonal variation of the deep-layer temperature at the basin station with the highest temperature in winter and lowest in summer is unusual, given the fact that intensive wintertime surface heat loss to the atmosphere in the GoM can drive convective mixing over much of the water column in winter (Mountain & Jessen, 1987; Mupparapu & Brown, 2002).

The unusual deep-layer temperature variation persisted over the entire 16 data-available years (Figure 6). The winter-summer temperature difference at 150 m has a mean of 1.5°C and a maximum of 2°C. The 42-years long NOAA hydrographic data set confirms that such unique seasonality exists not only in Jordan Basin but also in the neighboring Wilkinson Basin (Figure 7). This seasonal pattern differs distinctively from the neighboring shelves, such as the Mid-Atlantic Bight to the south (Linder & Gawarkiewicz, 1998; Zhang et al., 2011) and the Scotian Shelf to the north (Dever et al., 2016), where near-bottom temperature

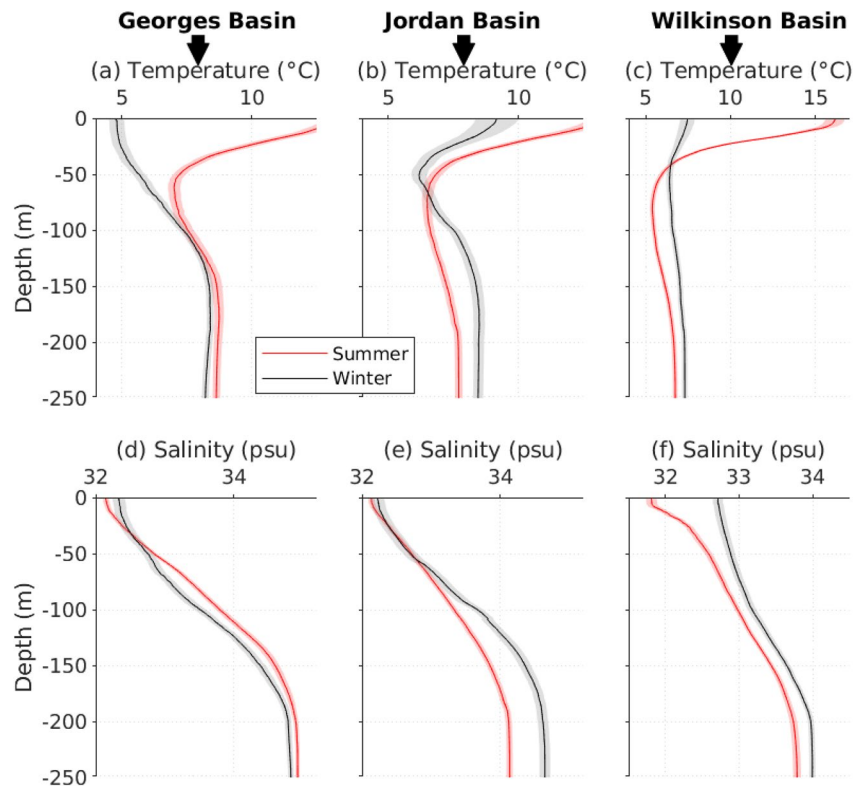


**Figure 7.** Summer and winter mean temperature and salinity profiles at Georges, Jordan, and Wilkinson Basins. The vertical profiles at each basin are computed from the 42-years (1977–2018) long NOAA hydrographic survey dataset. For each basin, vertical profiles within a 50 km radius from the basin centers are used. The coordinates of the basin centers are (42.70°N, 67.00°W), (43.49°N, 67.88°W), and (42.50°N, 69.50°W) for Georges, Jordan, and Wilkinson Basins, respectively (see Figure 1b for their locations). Summer months are June-August, and winter months are December-February. The colored shades indicate the standard error of the yearly mean.

follows a typical seasonal cycle, that is, being higher in summer and lower in winter. It also differs from the temperature profile at Georges Basin, which has a “normal” seasonal variation (Figure 7), similar to that at the NEC.

### 3.2. Timescale for Inner Gulf's Response

To establish the connection between the deep water at the basin station with that at the channel station, we computed the correlation of the temperature and salinity time series at the two stations with different time lags. Our analysis shows a significant lag-correlation between the 100-m temperature anomalies (after removing the season variation) at the channel station and the 150-m temperature anomalies at the basin station. The  $R^2$  reaches a maximum of 0.60 when the basin temperature is shifted forward by 86 days (Figures 8a and 8b). This indicates that temperature anomaly signals propagate from the channel to the basin in about 3 months. The lag-correlation analysis of the salinity anomalies (Figures 8c and 8d), and that of the full temperature and salinity signals (without removing the seasonal variation; Figures 8e–8h) give similar results. These indicate possible connections between the channel and the basin over seasonal to interannual time scales. It is noticeable that the amplitude of the temperature fluctuation is significantly reduced from the channel to the basin (Figure 3; Figure 8a). The weakening of temperature fluctuation from the channel source to the basin presumably reflects a gradual mixing of the intruding slope water with surrounding water masses.

Lagrangian particle tracking in the GoM numerical model confirms the lag timescale. Most of the modeled passive particles released at 100 m depth at the NEC follow the cyclonic circulation and move toward the gulf interior (Figure 9c). The median time for the particles to reach Jordan Basin for the first time is 90 days (Figure 9d), consistent with the observation-based advective timescale. It confirms a 3-months lag response of the interior gulf to variations of ocean conditions in the neighboring slope sea.

The tracks of the particles as shown in the probability map depicts the major route of the released particles (Figure 9b). Most of the released particles move into the gulf along the channel and then toward the inner gulf. A large number of particles move cyclonically along the rim of the deep basins following the 150 m isobath. Some of the particles reached Jordan Basin and then continue move westward along the basin rim. The movement pattern of the particles can be attributed to the deep circulation in the gulf (Figure 9c), which is featured by a gulf-wide cyclonic flow along the isobath and several smaller-scale eddy-like flow features.

### 3.3. Impact of Gulf Stream and Warm-Core Rings

The intruding subsurface slope water in the GoM originates from the slope sea off the NEC and has properties similar to Labrador Slope Water and Warm Slope Water (Figure 5). Presumably, the relative contributions of the two slope water masses depend on the competing influences of the Gulf Stream and Labrador Current (Gatién, 1976). The influence of the Gulf Stream on the slope water intruding into the GoM likely varies in coordination with its proximity to the NEC. As the Gulf Stream meanders and sheds warm-core rings into the slope sea, the distance between the NEC and the Gulf Stream water (including the ring water) changes dramatically in time. We here hypothesize that the proximity of the Gulf Stream water to the NEC affects conditions of the slope water intruding into the GoM.

Statistical analysis of a 26-years (1993–2018) SSH data set shows that the Gulf Stream is closest to the NEC in fall and furthest away from the NEC in February–April (Figures 10c–10e). This seasonal variation of the distance between the Gulf Stream and NEC is approximately in phase with the seasonal variation of the deep-layer temperature and salinity in the NEC: close Gulf Stream proximity to NEC corresponds to higher deep-layer temperature and salinity in the NEC. To further examine their relationship, we compared the monthly mean distance between the Gulf Stream and NEC with the monthly mean deep-layer salinity in the NEC (Figure 10f). There appears to be a significant negative relationship between the two. Because the Gulf Stream water is warmer and saltier than other water masses in the slope sea, this negative relationship is consistent with the hypothesized connection between the NEC-Gulf Stream distance and the slope water conditions in the NEC. That is, the statistical analysis suggests that closer proximity of the Gulf Stream to the NEC leads to higher salinity of the intruding slope water in the NEC. The dynamics responsible for this

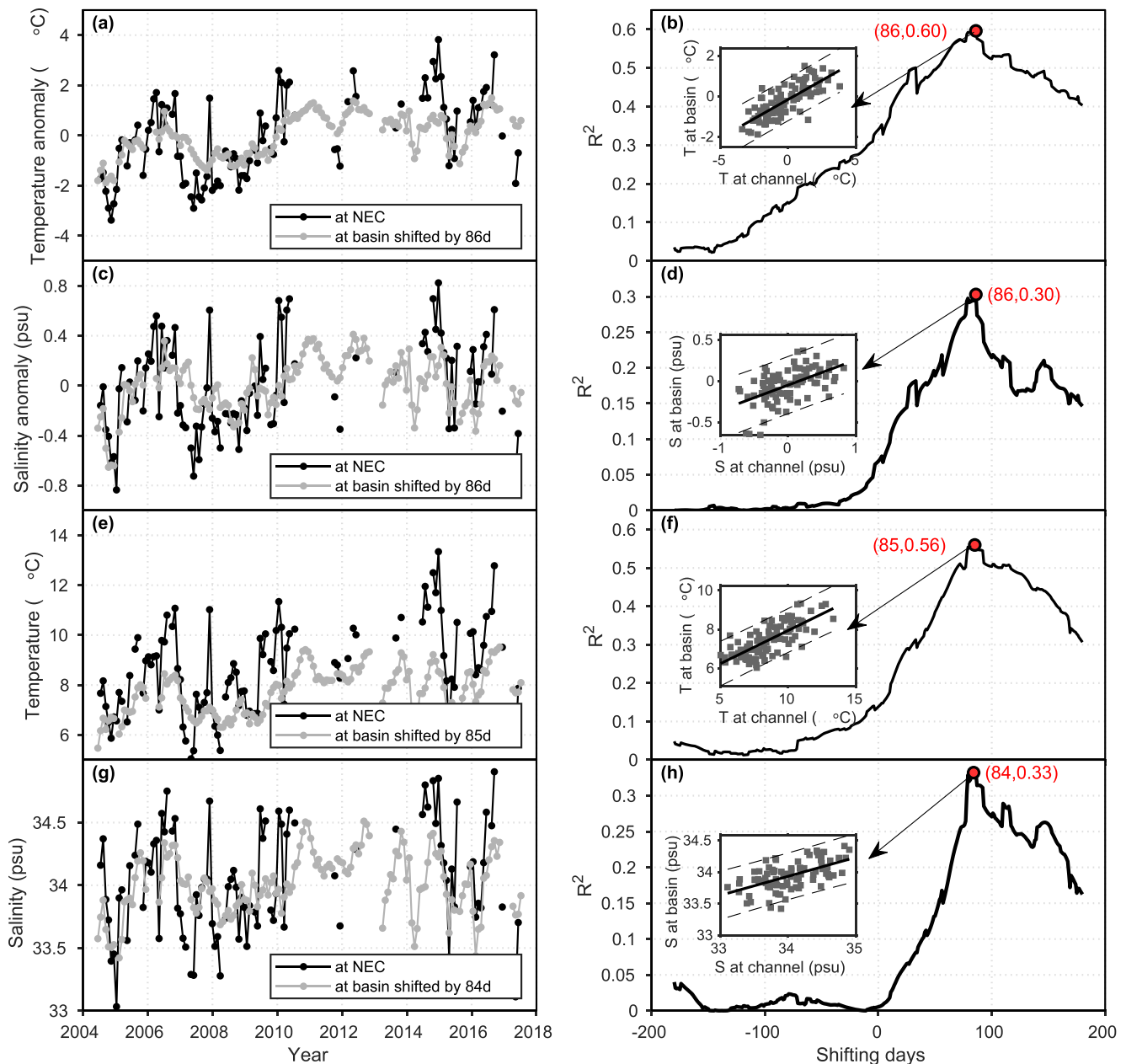


**Figure 8.** Delayed responses of the deep basin to changes at the shelf edge based on lag-correlation analysis of observed temperature, salinity, and their anomalies. (a) Monthly averaged deep-layer temperature anomaly at two stations; temperature at the basin station is shifted forward by 86 days (b) The  $R^2$  between the monthly averaged deep-layer temperature anomaly at two stations when shifting the basin temperature by different days; (c)–(d) are the same as (a)–(b) but for salinity anomaly; (e)–(f) for temperature and (g)–(h) for salinity. The insets in right panels show scatter plots of measured deep-layer temperature/salinity (or anomalies) at the channel station versus time-shifted deep-layer value at the basin station, and the lines represent linear fits and dashed lines indicate 95% confidence interval.

relationship, that is, the mechanism of the Gulf Stream influencing the slope water condition, remains unknown and will be discussed in Section 4.

Episodic warm-core rings shed from northward meanders of Gulf Stream could also have a drastic impact on the intruding water at the NEC. For instance, in August 2016, as a warm-core ring impinged onto the shelf edge next to the NEC (Figures 11a and 11c), the deep-layer (below 100 m) temperature and salinity at the channel station increased by  $4^{\circ}\text{C}$  and 3 psu, respectively (Figure 11e). Even stronger fluctuation in temperature and salinity at the NEC occurred during another ring impingement event in June of 2017

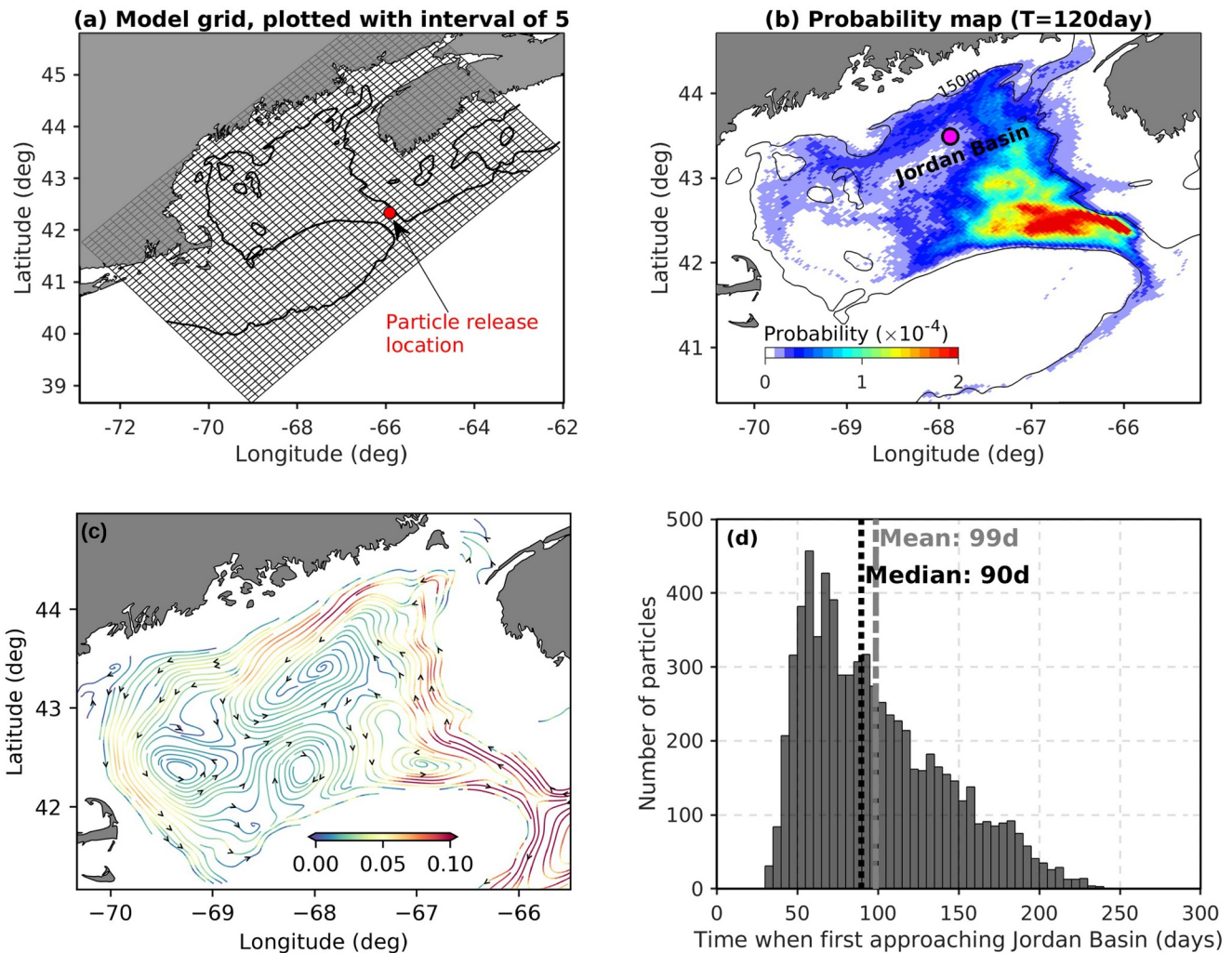


**Figure 9.** Numerical simulation results showing the transport pathway and timescale of water mass connectivity between the inner gulf and NEC. (a) Model grid, plotted with every 5 grids in both along- and cross-shelf directions. (b) The 120-days post-release probability map of particles released at the NEC. (c) Modeled mean summertime circulation at 100 m. (d) Histogram of the time of modeled particles released at the channel first reaching Jordan Basin. The black line in (b) is 150 m isobath contour.

(Figures 11b and 11d). The amplitude of the temperature fluctuation (4–5°C) is larger than the maximum seasonal difference (approximately 3°C, see Figure 4g). It is presumable that the dramatic cross-shelf exchange induced by the ring-topography interaction at the Mid-Atlantic Bight (e.g., Cherian & Brink, 2016; Zhang & Gawarkiewicz, 2015) could occur at the shelf edge off GoM. The dynamics of this ring-induced intrusion is not directly addressed in this study, but it will be discussed in Section 4.

### 3.4. Impact of Nova Scotia Current

In this section, we seek to understand how the temperature and salinity signal of the intruding slope water is preserved in the deep basin of the GoM. While moving inside the GoM, the intruding slope water is subject to the influence of lateral and vertical mixing with the surrounding waters. The mixing, driven by processes such as tides, eddies, and convection, could modify the properties of the intruding slope water. The observed smaller temperature fluctuation at depth at the basin station relative to the channel station (Figures 4c and 4g) likely reflects the influence of mixing. Another example is the discrepancy in the channel and basin conditions in 2016–2017: the 2016 fall season was featured with anomalously high deep-layer salinity in the channel compared to other years (Figure 12b), while the deep-layer salinity at the basin station in early 2017



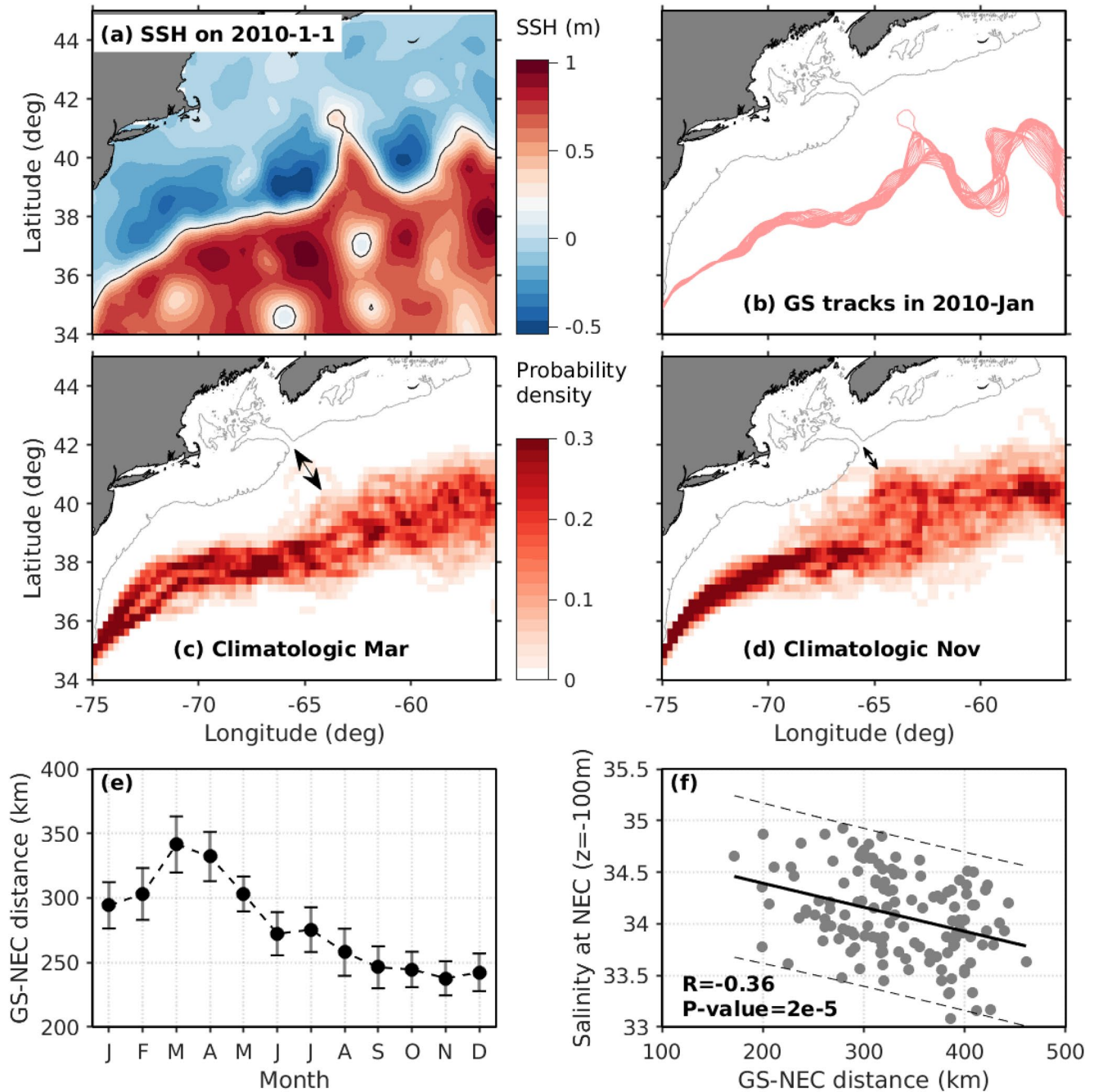


**Figure 10.** Impact of Gulf Stream proximity on the sub-surface salinity at the NEC. (a) A sample SSH map, with the contour of 25 cm highlighted with black lines. The longest 25 cm SSH contour is used to indicate the Gulf Stream path. (b) Gulf Stream paths in January 2010. (c)–(d) The probability of Gulf Stream passing through sub-regions of  $1/4 \times 1/4^\circ$  in March and November, respectively, highlighting the much closer proximity of Gulf Stream to NEC in November. (e) Seasonality of the minimum distance between Gulf Stream and NEC, with the error bars indicating the standard error of monthly mean. (f) The negative correlation (with coefficient  $R$ ) between monthly mean Gulf Stream–NEC distance and monthly mean bottom salinity at NEC, with the black solid line showing a linear least-squared fit and black dashed lines indicating the 95% confidence intervals.

(3 months later) was merely near the long-term mean (Figure 12c). Such discrepancy implies a confounding impact of local gulf processes on the intruding slope water presumably through mixing.

One major factor that could affect the deep water condition in the GoM is vertical convection. Observations have shown that wintertime surface heat loss to the cold atmosphere could drive vertical convection and mixing, which then ventilates the deep water in the gulf basin and modify its properties (Mupparapu &

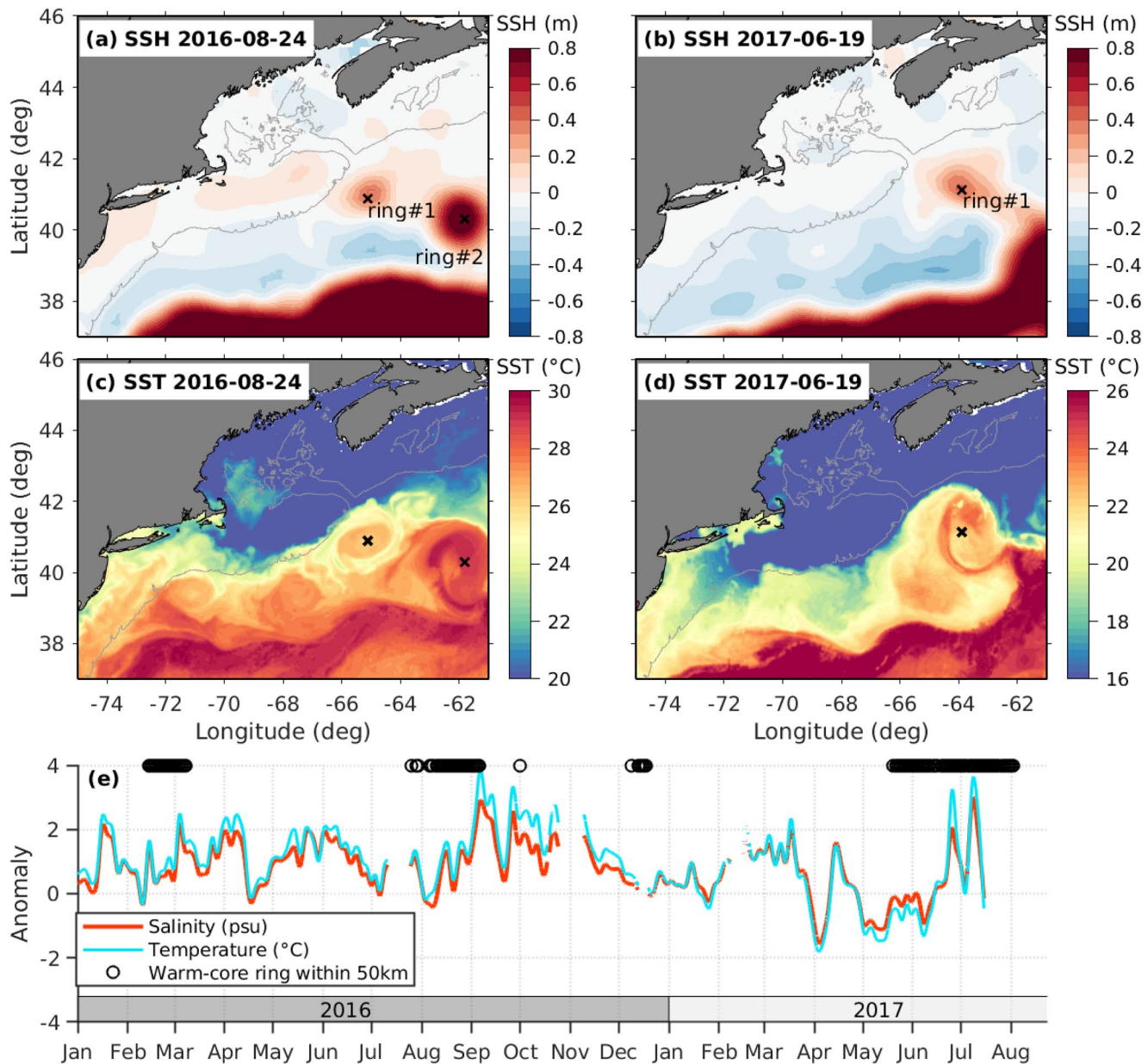


**Figure 11.** Impact of warm-core rings on the deep water at the NEC. (a–b) SSH maps on 24/8/2016 and 19/6/2017 with automatically detected ring centers marked with black crosses. (c–d) SST images on the same days showing warm-core rings impinging onto the shelf edge. (e) Time series of subsurface temperature and salinity anomalies at the channel station, averaged over the water column below 100 m depth. Circles in (e) denote the presence of a warm-core ring within 50 km away to the NEC.

Brown, 2002). Brown and Beardsley (1978) demonstrated that the occurrence of wintertime vertical convection in the GoM depended highly on the surface salinity and that vertical convection was only noticeable in years with high surface salinity. This influence of the surface salinity presumably reflects the effect of near-surface stratification on vertical mixing.

One major freshwater source contributing to the lower surface salinity in the inner gulf is the Nova Scotia Current. Nova Scotia Current is an equatorward buoyancy-driven coastal current forced by upstream glacial melt and river runoff along the northeast coast of North America (Chapman & Beardsley, 1989). It carries a large amount of freshwater into the GoM and reaches its maximum strength in winter (Smith, 1983). Long-term survey data on the Scotian Shelf give a mean cross-shelf salinity of  $S = 32$  psu in the top 100 m (Dever

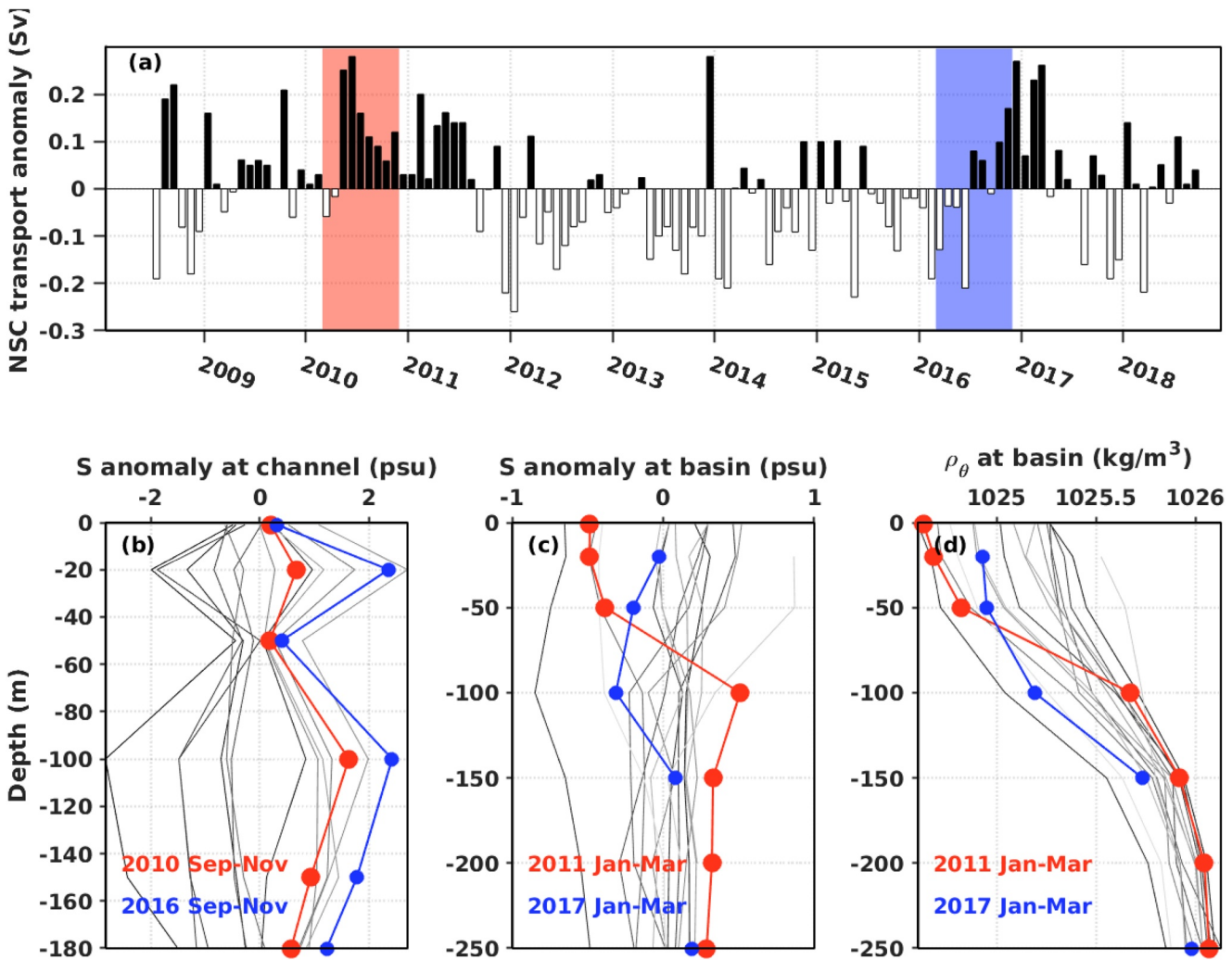


**Figure 12.** Impact of Nova Scotia Current on the GoM interior. (a) Time series of Nova Scotia Current transport anomaly. (b) Mean salinity anomaly profiles in the NEC averaged over September–November of each year; (c) mean salinity anomaly profiles in Jordan Basin averaged over January–March of each year; and (d) mean potential density profiles in Jordan Basin averaged over January–March of each year.

et al., 2016) and a seasonally maximum along-shelf transport ( $Q_s$ ) in wintertime of 0.61 Sv (Hebert, Pettipas, Brickman, et al., 2013). Assuming an ambient ocean salinity ( $S_0$ ) of 34 psu, the wintertime freshwater transport in the Nova Scotia Current,  $Q_f = Q_s(S_0 - S)/S_0 = 3.6 \times 10^4 \text{ m}^3/\text{s}$ , which is more than three times of the seasonal maximum of freshwater input from all rivers feeding into the GoM of  $1 \times 10^4 \text{ m}^3/\text{s}$  (Li, He, & McGillicuddy, 2014). Therefore, the freshwater input from the Nova Scotia Current dominates the surface salinity in the GoM.

Because surface salinity in the GoM affects the wintertime convection, the freshwater and buoyancy input from the Nova Scotia Current likely affects properties of the deep water in the gulf basin. We here hypothesize that a large buoyancy input from the Nova Scotia Current into the GoM enhances near-surface stratification and suppresses vertical mixing in the deep basin, which tends to preserve the temperature and salinity signals of the intruding slope water at depth. To test this hypothesis, we analyzed 10-years (2008–2018) continuous ADCP velocity measurements across the inner Scotian Shelf at Halifax, Canada (Dever et al., 2016; Hebert, Pettipas, & Brickman, 2020). Anomalies of the Nova Scotia Current transport relative to the 10-years seasonal mean show a significant negative correlation with the measured surface salinity at the basin station (Figure 13b). The maximum correlation is achieved when the surface salinity anomaly is shifted forward by 35 days and the Nova Scotia Current transport is averaged over a 9-month window prior to the basin station measurement (Figure 13a). That is, the mean Nova Scotia Current transport in the 1st



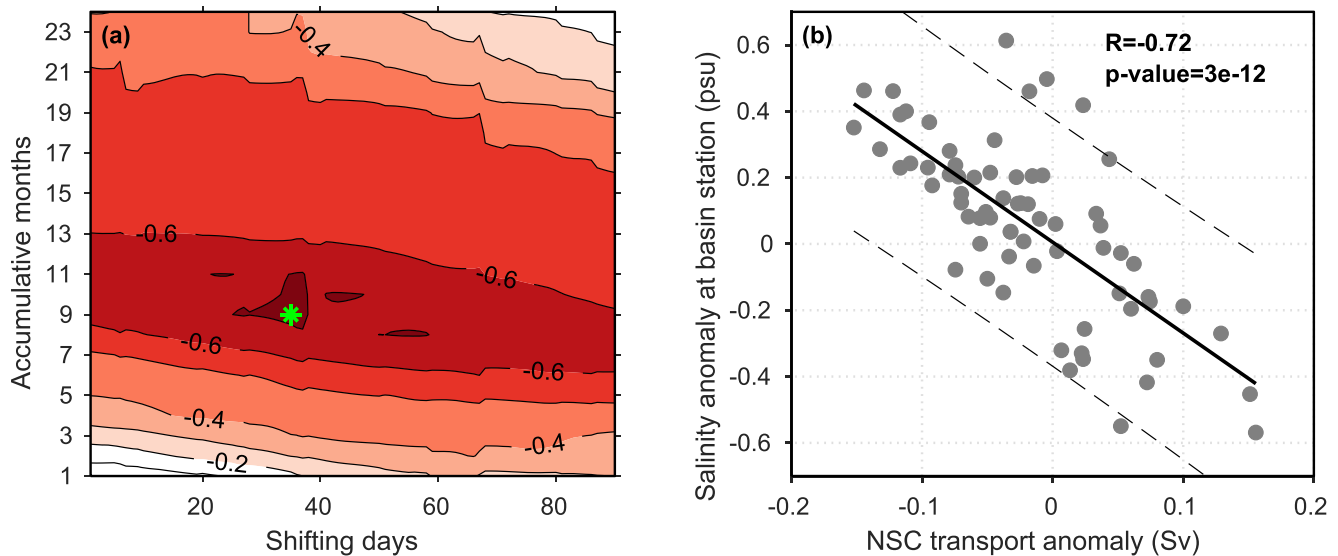


**Figure 13.** (a) Contour plot of correlation coefficient ( $R$ ) between accumulatively averaged Nova Scotia Current transport and forward-shifted mean surface salinity (0–50m) observed at the basin station, with the green asterisk denoting the highest  $R$  obtained when shifting salinity forward by 35 days and accumulating Nova Scotia Current transport in the prior 9 months (b) The linear relationship between the Nova Scotia Current transport and the surface salinity anomaly at the basin station at the highest  $R$ , with the black solid line showing a linear least-squared fit and black dashed lines indicating the 95% confidence interval.

to the 9th month is highly related to the mean surface salinity of the 10th month at the basin. It implies an accumulative impact of the Nova Scotia Current input on the basin surface salinity. The 1-month time lag is consistent with the advection time over the 400 km distance from Halifax to Jordan Basin, assuming a mean flow on the order of  $10 \text{ cm s}^{-1}$  (Dever et al., 2016; Smith et al., 2001). The 9-months averaging window is empirically obtained from the correlation analysis and likely reflects the mixing that the water flowing from the Nova Scotia Shelf to the inner GoM is subjected to. While the leading edge of flow signal could reach the basin within a month, water in the flow pathway constantly mixes with the surrounding waters that have been shed from the flow in the past. Therefore, the salinity condition at Jordan Basin likely reflects a temporally integrated signal of the upstream condition on the Nova Scotian Shelf.

We now seek to establish the connection between the Nova Scotia Current transport and the GoM deep water. Lag-correction analysis of the available 10-years data shows *no* significant correlation between the Nova Scotia Current transport anomalies and the deep-layer temperature at the basin station. This is not surprising, as any influence of the Nova Scotia Current on the *deep* gulf water would be indirect: it requires the intermediate step of affecting *surface* salinity in the basin and the joint influence of cold wintertime air temperature. In particular, the deep gulf water is affected by multiple factors, including (i) the slope water condition, (ii) the strength of the slope water intrusion, (iii) the Nova Scotia Current transport, and (iv) the episodic wintertime convection in the gulf. The influence of the first two factors are more direct and continuous, while that of the last two factors are interconnected and event-driven. Therefore, it likely needs a longer time series covering a number of strong winter convection events to show a statistically significant relationship between the Nova Scotia Current and the deep gulf water condition. A close examination of the available data does show the episodic impact from the Nova Scotia Current. For instance, there was a major positive Nova Scotia Current transport anomaly (i.e., more freshwater input into the GoM) over the period of May–November 2010 (the red patch in Figure 12a). Consistently, at the basin station in January–March 2011, the measured surface salinity was anomalously low (Figure 12c); the stratification at 50–100 m below the surface was anomalously strong (Figure 12d); and the deep-layer salinity was the highest in the 16 data-available years (the red line in Figure 12c), even though the salinity of the source slope water at the NEC 3 months prior was not the highest (Figure 12b). Note that the deep-layer temperature at the basin station in January–March 2011 was also the highest in the 16 years (not shown). Therefore, consistent with Brown and Beardsley's (1978) finding, a strong freshwater input from the Nova Scotia Current to the surface GoM likely



enhances the near-surface stratification, suppresses the wintertime deep convection, and helps to preserve properties of the intruding slope water in the deep basin.

Because the deep convection could only occur in wintertime, timing of the surface freshwater input into the GoM is important. A strong Nova Scotia Current freshwater input could help preserve the properties of the intruding slope water in the deep basin *only if* the freshwater reaches the surface layer of the basin in the winter when convection could occur. This explains the deep-layer salinity in the basin in January–March 2017 being at its long-term mean level (the blue line in Figure 12c), even though the measured Nova Scotia Current freshwater transport is anomalously positive over the period of October 2016–March 2017. Note that the mean Nova Scotia Current transport in April 2016–November 2016, the 9 months prior to January 2017, was only slightly above its long-term mean level (the blue patch in Figure 12a). That is, the anomalously high freshwater flow from the Scotian Shelf during October 2016–March 2017 did not reach Jordan Basin early enough to suppress the wintertime convection there, and its influence was confounded by the weak transport in the earlier months of April–September 2016.

#### 4. Discussion

In this section, we discuss the connection of the flow in the NEC with the slope water intrusion into the GoM and propose a few potential mechanisms of Gulf Stream and warm-core rings influencing the slope water intrusion. We first analyze the intrusion flow at the NEC by examining the ADCP-measured velocity. Flow in the NEC is dominated by tides, as the depth-averaged velocity shows a tidal ellipse with a major axis of approximately  $0.7 \text{ m s}^{-1}$ , oriented  $45^\circ$  to the northwest along the channel (Figure 14a). The long-term mean of the depth-averaged velocity was primarily along-channel, and we thus focus the following analysis on the along-channel component of the velocity. The vertical profile of the along-channel velocity averaged over the 14 ADCP-available years (2004–2017) show a net inflow throughout the water column and a subsurface maximum inflow of  $8 \text{ cm s}^{-1}$  at 50 m below surface (Figure 14b). The inflow decreases gradually from the maximum toward the bottom. This indicates the intrusion flow is a vertically persistent feature in the channel.

The intrusion flow varies in time. Time series of the monthly-averaged along-channel velocity show temporal variability over a variety of time scales (Figure 14d). The seasonal climatology of the along-channel flow shows a seasonal variation with a summertime maximum inflow in most of the water column, except the top 50 m. This seasonal variation of the inflow velocity is generally in phase with the variation of the subsurface temperature and salinity in the channel (Figures 4e–4g). In particular, the subsurface temperature, salinity, and inflow in the channel all reach their peaks in August–September. There is a weak mean bottom outflow in the period of November–March. The general synchronicity between the intrusion velocity and hydrographic conditions of the intruding slope water occurs not only on the seasonal time scale. Figure 14e shows a positive relationship between the monthly mean subsurface inflow velocity and the monthly mean deep-layer density at the channel over the data-available years. The coincidence of strong inflow and high temperature and salinity in the channel provides an efficient way of transporting heat and salt from the slope sea into the gulf. It is likely that this coincidence reflects stronger inflow carrying higher temperature and higher salinity slope water into the channel. However, it is also possible that the temporal variation of the temperature and salinity of the intruding water reflected changes in the slope sea conditions, which then modifies the intensity of the intrusion flow through local baroclinic processes. The specific mechanism of the coincidence remains unknown. But this type of temporal variation of the channel flow and hydrographic condition is likely connected to the open ocean processes that we have identified.

With a statistical analysis of the available observational data, we have established the connection between Gulf Stream activities and the slope water intrusion into the NEC and then the deep water in Jordan Basin. However, the available data are not enough for studying the dynamics of how Gulf Stream influences the slope water intrusion. To achieve a mechanistic understanding of the open ocean influence on the deep water in the GoM would require either a more comprehensive set of observational data or a specifically designed numerical model. The model would have to have a resolution high enough to capture fine-scale details of the intrusion process in the GoM and at the same time include the large-scale open ocean processes. This is beyond the capability of the GoM model we have used here for the particle tracking. Designing a

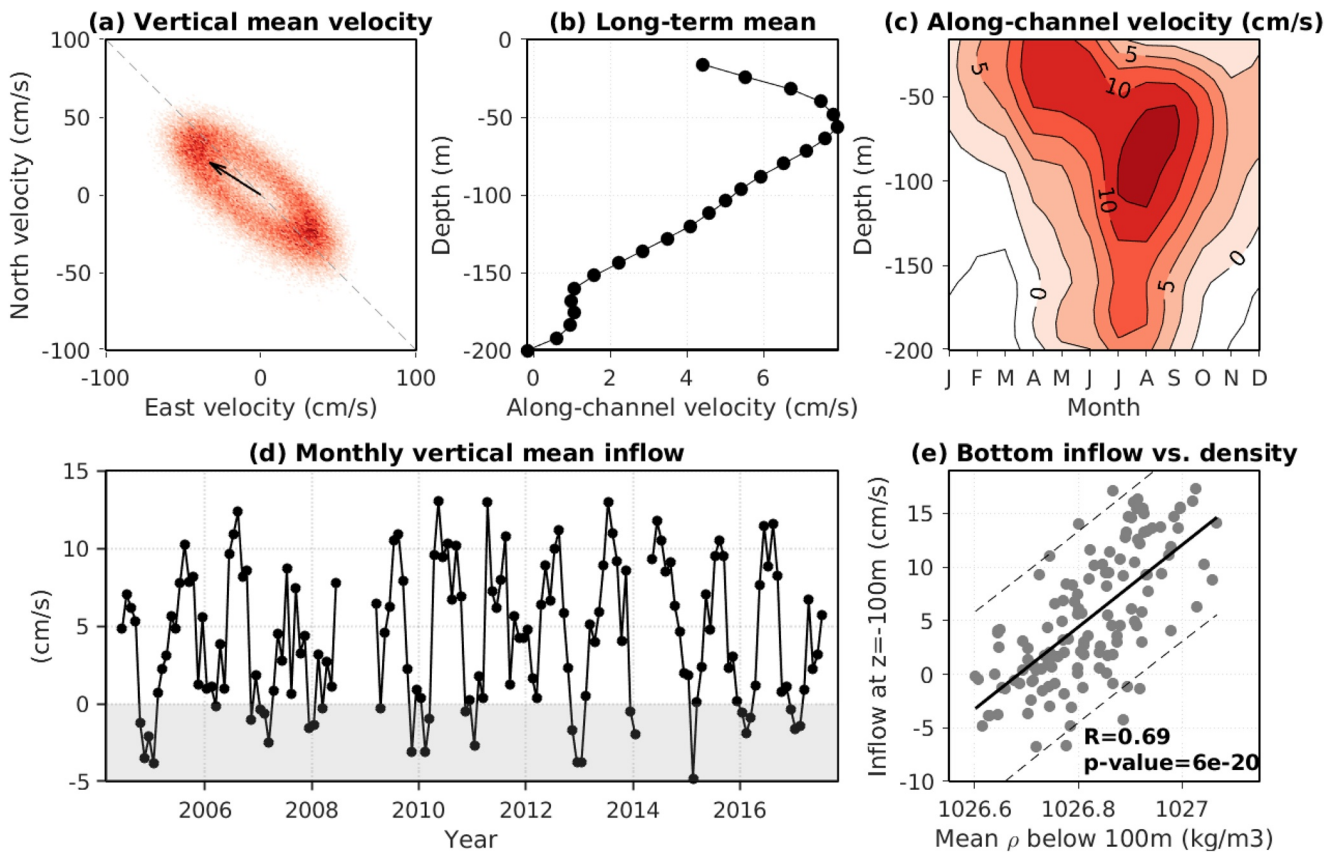


**Figure 14.** ADCP-measured velocity at the NEC. (a) Probability density distribution of vertically averaged velocity (tidal currents are included), with redder color denoting a higher probability density. The black arrow in (a) denotes the direction of long-term mean vertically averaged velocity. (b) The vertical profile of long-term mean along-channel velocity, with positive value indicating inflow toward the GoM. (c) Seasonal variation of the along-channel velocity. (d) Time series of monthly mean vertically averaged inflow, only showing the months with less than 20% of data gaps. (e) Relationship of monthly mean along-channel velocity at 100 m with mean density below the 100 m depth in the NE, with the black solid line showing a linear least-squared fit and black dashed lines indicating the 95% confidence interval.

new model to investigate the dynamics of the open ocean influence is an ongoing research, which is beyond the scope of this work. Nevertheless, we here provide some speculations on the mechanisms of Gulf Stream impacting the slope water intrusion into the GoM.

The relationship between the proximity of the Gulf Stream to the NEC and properties of the intruding slope water in the NEC identified here could be facilitated by either latitudinal shift in the mean position of the Gulf Stream or its meanders or eddy activities. Frankignoul et al. (2001) showed that the latitudinal position of the Gulf Stream varies with North Atlantic Oscillation (NAO). In particular, 11–18 months after the NAO reaches the positive extrema, the Gulf Stream tends to shift northward. This would result in a closer proximity between the Gulf Stream and the NEC, leading to a stronger influence of Gulf Stream on the slope water intrusion in the GoM. Meanwhile, instability activities of the Gulf Stream vary over the seasonal time scale with the highest eddy kinetic energy below 100 m occurring in September (Kang et al., 2016). Note that the eddy kinetic energy is the difference between the total and mean kinetic energy, and thus contains all perturbation energy, including meanders and eddies (e.g., warm-core rings). Consistently, analysis of 38-years of satellite-data based Gulf Stream charts reveals that warm-core ring formations have a maximum in summer and minimum in winter (Gangopadhyay et al., 2020). More active Gulf Stream meanders or eddies in the summer would cause wider lateral spread of the Gulf Stream water, which on average would result in a stronger influence of the Gulf Stream on the slope sea and modify the slope water condition near the NEC. This seasonal variation in the eddy activities could thus be the underlying mechanism responsible for the summer maxima of temperature, salinity, and shoreward intrusion at the bottom of the NEC.

The dynamics of Gulf Stream affecting the slope water intrusion remains unclear. Presumably, Gulf Stream could impact the intruding slope water in the NEC through different mechanisms, such as (1) enhancing the volume of slope water intruding into the channel, (2) increasing temperature and salinity of the intruding slope water, and (3) direct intrusion of the Gulf Stream or ring water into the channel. First, as the Gulf Stream or warm-core rings move closer to the NEC, they could push more slope water into the channel through either (i) raising the sea level in the slope sea and driving more subsurface inflow in the topographically constrained channel, or (ii) inducing a northeastward slope current, which could then generate upwelling of the subsurface slope water into the channel. The former process results from the enhanced barotropic cross-shelf pressure gradient, and the latter process is similar to the upwelling flow in a slope canyon resulting from an ambient flow opposing the propagation of coastal-trapped waves (e.g., Allen & Durrieu de Madron, 2009; Zhang & Lentz, 2017). Second, northward shifted Gulf Stream or warm-core rings, through mixing, could increase the temperature and salinity of the slope water either near the NEC or farther upstream off the Scotian shelf (Brinkman et al., 2018), which could then be advected into the NEC and alter the deep water properties in the deep GoM. Last, when a warm-core ring impinges onto the shelf edge close to the NEC, shallow limbs of the ring could carry the warm and salty ring water intruding directly into the NEC, similar to the onshore intrusion of the ring water onto the neighboring Mid-Atlantic Bight continental shelf (Zhang & Gawarkiewicz, 2015). Which one(s) of these proposed mechanisms occur in the real ocean remains unclear and is left for future studies.

Large-scale atmospheric variabilities, particularly the NAO, play an essential role in regulating the regional oceanic conditions and may also affect the deep water in the GoM. The NAO modulates not only the Gulf Stream position (Frankignoul et al., 2001; Taylor & Stephens, 1998) but also the Labrador Current as well as the predominance of the two slope water masses off the Scotian Shelf (Petrie, 2007). A sustained low NAO is associated with increased transport of the Labrador Current and colder and fresher water on the downstream shelf (Greene & Pershing, 2003; Brickman, et al., 2018). For instance, an extreme low of the NAO in 2010 and 2011 coincided with the anomalously stronger transport of the Nova Scotia Current (Hebert, Pettipas, & Brickman, 2020), which may have caused the anomalously fresh condition in the surface layer and the strongly stratified water column at Jordan Basin in early 2011 (Figures 12c and 12d).

## 5. Summary

Based on a comprehensive data set, we examined the variability of the bottom water in the GoM and show observational evidences of open ocean processes impacting this semi-enclosed shelf sea. Major results are summarized as below.

1. Long-term continuous monitoring data show the deep-layer temperature in the GoM is persistently higher in winter than in summer. This unique seasonal variation of temperature of the deep water in the GoM is a lagged response ( $\sim 3$  months) to the seasonally varying slope water condition off the NEC, and that the 3-months delay reflects the advection time of the intrusion flow from the channel to the deep gulf basin.
2. The interannual and seasonal variabilities of the GoM bottom water are determined by open ocean processes and affected by local mixing processes.
3. The Gulf Stream activities affect the source properties of the intruding slope water. Episodic Gulf Stream warm-core rings in the region can also drastically increase the temperature and salinity of the intruding slope water.
4. Surface freshwater input from the upstream Scotian Shelf into the GoM helps to preserve properties of the intruding slope water in the deep basin of the GoM by enhancing near-surface stratification and suppressing wintertime vertical ventilation.

Dynamics of the open ocean influence, such as mechanism of Gulf Stream influencing the slope water off the NEC and dynamics of the slope water intruding into the bathymetrically constrained NEC, remain to be further explored. This study provides a clear demonstration of the influence of open ocean processes on a

coastal system. Findings here have implications on the regional ecosystem, as the intruding slope water provides a large amount of nutrients to sustain the high productivity in the GoM. By affecting the slope water mass and intrusion strength, open ocean processes could impact biological productivity in this unique shelf sea. Meanwhile, due to the strong seasonality in surface-layer nutrient availability and biological production, timing of both horizontal advection and vertical mixing are key aspects of the biophysical coupling in the GoM. Our results on the temporal variability of open ocean influences, the time scales of the advective processes, and the intermittency of the convective mixing process will help us better understand the biological productivity and ecosystem dynamics in the GoM.

### Data Availability Statement

The long-term mooring data at the Jordan Basin and Northeast Channel stations were downloaded from the publicly accessible data server ([http://www.neracoos.org/thredds/UMO\\_SOS\\_historical\\_realtime\\_agg.html](http://www.neracoos.org/thredds/UMO_SOS_historical_realtime_agg.html)) maintained by Northeastern Regional Association of Coastal Ocean Observing Systems. The NOAA historical hydrographic survey data were downloaded from the publicly accessible data server at [https://comet.nefsc.noaa.gov/erddap/tabledap/nefsc\\_ctd.html](https://comet.nefsc.noaa.gov/erddap/tabledap/nefsc_ctd.html). We thank James Manning for his help in providing the NOAA survey data. The measured Nova Scotia Current transport along the Halifax line across the Scotian Shelf is based on figure 34 in Hebert, Pettipas, and Brickman (2020). Satellite data of sea surface temperature are produced by Jet Propulsion Laboratory (data publicly accessible at <https://coastwatch.pfeg.noaa.gov/erddap/griddap/jplG1SST.html>). Gridded daily satellite altimetry data were download from the public server of European Union Copernicus Marine Environmental Monitoring Service (<https://cds.climate.copernicus.eu/cdsapp#!/dataset/satellite-sea-level-global?tab=overview>).

### Acknowledgments

This study is supported by the National Science Foundation through grant OCE 1634965.

### References

- Allen, S. E., & Durrieu de Madron, X. (2009). A review of the role of submarine canyons in deep-ocean exchange with the shelf. *Ocean Science*, 5(4), 607–620. <https://doi.org/10.5194/os-5-607-2009>
- Andres, M. (2016). On the recent destabilization of the Gulf Stream path downstream of Cape Hatteras. *Geophysical Research Letters*, 43(18), 9836–9842. <https://doi.org/10.1002/2016GL069966>
- Bigelow, H. B. (1927). Physical oceanography of the Gulf of Maine. *Bulletin of the US Bureau of Fisheries*, 40, 511–1027.
- Bisagni, J. J., & Smith, P. C. (1998). Eddy-induced flow of Scotian Shelf water across Northeast Channel, Gulf of Maine. *Continental Shelf Research*, 18(5), 515–539. [https://doi.org/10.1016/S0278-4343\(98\)00001-6](https://doi.org/10.1016/S0278-4343(98)00001-6)
- Brickman, D., Hebert, D., & Wang, Z. (2018). Mechanism for the recent ocean warming events on the Scotian Shelf of eastern Canada. *Continental Shelf Research*, 156, 11–22. <https://doi.org/10.1016/j.csr.2018.01.001>
- Brink, K. H. (2016). Cross-Shelf Exchange. *Annual Review of Marine Sciences*, 8(1), 59–78. <https://doi.org/10.1146/annurev-marine-010814-015717>
- Brown, W. S., & Beardsley, R. C. (1978). Winter Circulation in the Western Gulf of Maine: Part 1. Cooling and Water Mass Formation. *Journal of Physical Oceanography*, 8(2), 265–277. [https://doi.org/10.1175/1520-0485\(1978\)008<0265:WCITWG>2.0.CO;2](https://doi.org/10.1175/1520-0485(1978)008<0265:WCITWG>2.0.CO;2)
- Chapman, D. C., & Beardsley, R. C. (1989). On the Origin of Shelf Water in the Middle Atlantic Bight. *Journal of Physical Oceanography*, 19(3), 384–391. [https://doi.org/10.1175/1520-0485\(1989\)019<0384:OTOOSW>2.0.CO;2](https://doi.org/10.1175/1520-0485(1989)019<0384:OTOOSW>2.0.CO;2)
- Chaudhuri, A. H., Gangopadhyay, A., & Bisagni, J. J. (2009). Interannual variability of Gulf Stream warm-core rings in response to the North Atlantic Oscillation. *Continental Shelf Research*, 29(7), 856–869. <https://doi.org/10.1016/j.csr.2009.01.008>
- Chelton, D. B., Schlax, M. G., Samelson, R. M., & de Szoeke, R. A. (2007). Global observations of large oceanic eddies. *Geophysical Research Letters*, 34(15). <https://doi.org/10.1029/2007GL030812>
- Cherian, D. A., & Brink, K. H. (2016). Offshore Transport of Shelf Water by Deep-Ocean Eddies. *Journal of Physical Oceanography*, 46(12), 3599–3621. <https://doi.org/10.1175/JPO-D-16-0085.1>
- Cornillon, P. (1986). The Effect of the New England Seamounts on Gulf Stream Meandering as Observed from Satellite IR Imagery. *Journal of Physical Oceanography*, 16(2), 386–389. [https://doi.org/10.1175/1520-0485\(1986\)016<0386:TEOTNE>2.0.CO;2](https://doi.org/10.1175/1520-0485(1986)016<0386:TEOTNE>2.0.CO;2)
- Csanady, G. T. (1979). The birth and death of a warm core ring. *Journal of Geophysical Research*, 84(C2), 777–780. <https://doi.org/10.1029/JC084iC02p00777>
- Dever, M., Hebert, D., Greenan, B. J. W., Sheng, J., & Smith, P. C. (2016). Hydrography and Coastal Circulation along the Halifax Line and the Connections with the Gulf of St. Lawrence. *Atmosphere-Ocean*, 54(3), 199–217. <https://doi.org/10.1080/07055900.2016.1189397>
- Fairall, C. W., Bradley, E. F., Hare, J. E., Grachev, A. A., & Edson, J. B. (2003). Bulk Parameterization of Air-Sea Fluxes: Updates and Verification for the COARE Algorithm. *Journal of Climate*, 16(4), 571–591. [https://doi.org/10.1175/1520-0442\(2003\)016<0571:BPOASF>2.0.CO;2](https://doi.org/10.1175/1520-0442(2003)016<0571:BPOASF>2.0.CO;2)
- Feng, D., & Hodges, B. R. (2020). The oil spill transport across the shelf-estuary interface. *Marine Pollution Bulletin*, 153, 110958. <https://doi.org/10.1016/j.marpolbul.2020.110958>
- Frankignoul, C., de Coëtlogon, G., Joyce, T. M., & Dong, S. (2001). Gulf Stream Variability and Ocean-Atmosphere Interactions. *Journal of Physical Oceanography*, 31(12), 3516–3529. [https://doi.org/10.1175/1520-0485\(2002\)031<3516:GSVAOA>2.0.CO;2](https://doi.org/10.1175/1520-0485(2002)031<3516:GSVAOA>2.0.CO;2)
- Gangopadhyay, A., Gawarkiewicz, G., Silva, E. N. S., Monim, M., & Clark, J. (2019). An observed regime shift in the formation of warm core rings from the Gulf Stream. *Scientific Reports*, 9, 12319. <https://doi.org/10.1038/s41598-019-48661-9>
- Gangopadhyay, A., Gawarkiewicz, G., Silva, E. N. S., Silver, A. M., Monim, M., & Clark, J. (2020). A Census of the Warm-Core Rings of the Gulf Stream: 1980–2017. *Journal of Geophysical Research: Oceans*, 125(8), e2019JC016033. <https://doi.org/10.1029/2019JC016033>
- Gatien, M. G. (1976). A Study in the Slope Water Region South of Halifax. *Journal of the Fisheries Board of Canada*, 33(10), 2213–2217. <https://doi.org/10.1139/f76-270>



- Greene, C. H., & Pershing, A. J. (2003). The flip-side of the North Atlantic Oscillation and modal shifts in slope-water circulation patterns. *Limnology & Oceanography*, 48(1), 319–322. <https://doi.org/10.4319/lo.2003.48.1.0319>
- Halliwel, G. R., & Mooers, C. N. K. (1983). Meanders of the Gulf Stream Downstream from Cape Hatteras 1975–1978. *Journal of Physical Oceanography*, 13(7), 1275–1292. [https://doi.org/10.1175/1520-0485\(1983\)013<1275:MOTGSD>2.0.CO;2](https://doi.org/10.1175/1520-0485(1983)013<1275:MOTGSD>2.0.CO;2)
- He, R., McGillicuddy, D. J., Keafer, B. A., & Anderson, D. M. (2008). Historic 2005 toxic bloom of Alexandrium fundyense in the western Gulf of Maine: 2. Coupled biophysical numerical modeling. *Journal of Geophysical Research*, 113(C7). <https://doi.org/10.1029/2007JC004602>
- Hebert, D., Pettipas, R., & Brickman, D. (2020). *Physical oceanographic conditions on the Scotian shelf and in the gulf of Maine during 2018*. Canadian Science Advisory Secretariat Research Document.
- Hebert, D., Pettipas, R., Brickman, D., & Dever, M. (2013). *Meteorological, sea ice and physical oceanographic conditions on the Scotian shelf and in the gulf of Maine during 2012*. Canadian Science Advisory Secretariat Research Document. <https://doi.org/10.1109/icdar.2013.236.2013/058>
- Hopkins, T. S., & Garfield, N., III. (1979). Gulf of Maine Intermediate Water. *Journal of Marine Research*, 37, 103–139.
- Houghton, R. W., & Fairbanks, R. G. (2001). Water sources for Georges Bank. *Deep Sea Research Part II: Topical Studies in Oceanography*, 48, 95–114. [https://doi.org/10.1016/S0967-0645\(00\)00082-5](https://doi.org/10.1016/S0967-0645(00)00082-5)
- Isern-Fontanet, J., García-Ladona, E., & Font, J. (2003). Identification of Marine Eddies from Altimetric Maps. *Journal of Atmospheric and Oceanic Technology*, 20(5), 772–778. [https://doi.org/10.1175/1520-0426\(2003\)20<772:IOMEFA>2.0.CO;2](https://doi.org/10.1175/1520-0426(2003)20<772:IOMEFA>2.0.CO;2)
- Joyce, T. M., Bishop, J. K. B., & Brown, O. B. (1992). Observations of offshore shelf-water transport induced by a warm-core ring. *Deep Sea Research Part A. Oceanographic Research Papers*, 39, S97–S113. [https://doi.org/10.1016/S0198-0149\(11\)80007-5](https://doi.org/10.1016/S0198-0149(11)80007-5)
- Kang, D., Curchitser, E. N., & Rosati, A. (2016). Seasonal Variability of the Gulf Stream Kinetic Energy. *Journal of Physical Oceanography*, 46(4), 1189–1207. <https://doi.org/10.1175/JPO-D-15-0235.1>
- Lai, D. Y., & Richardson, P. L. (1977). Distribution and Movement of Gulf Stream Rings. *Journal of Physical Oceanography*, 7(5), 670–683. [https://doi.org/10.1175/1520-0485\(1977\)007<0670:DAMOGS>2.0.CO;2](https://doi.org/10.1175/1520-0485(1977)007<0670:DAMOGS>2.0.CO;2)
- Li, Y., He, R., & McGillicuddy, D. J. (2014). Seasonal and interannual variability in Gulf of Maine hydrodynamics: 2002–2011. *Deep Sea Research Part II: Topical Studies in Oceanography*, 103, 210–222. <https://doi.org/10.1016/j.dsr2.2013.03.001>
- Li, Y., He, R., McGillicuddy, D. J., Anderson, D. M., & Keafer, B. A. (2009). Investigation of the 2006 Alexandrium fundyense bloom in the Gulf of Maine: In-situ observations and numerical modeling. *Continental Shelf Research*, 29(17), 2069–2082. <https://doi.org/10.1016/j.csr.2009.07.012>
- Lillibridge, J. L., & Mariano, A. J. (2013). A statistical analysis of Gulf Stream variability from 18+ years of altimetry data. *Deep Sea Research Part II: Topical Studies in Oceanography*, 85, 127–146. <https://doi.org/10.1016/j.dsr2.2012.07.034>
- Linder, C. A., & Gawarkiewicz, G. (1998). A climatology of the shelfbreak front in the Middle Atlantic Bight. *Journal of Geophysical Research*, 103(C9), 18405–18423. <https://doi.org/10.1029/98JC01438>
- Mertz, F., & Legeais, J. F. (2020). *Product user Guide and Specification sea level v1.2*. ECMWF Copernicus Rerpot. Retrieved from [https://datastore.copernicus-climate.eu/documents/satellite-sea-level/D3.SL.1-v1.2\\_PUGS\\_of\\_v1DT2018\\_SeaLevel\\_products\\_v2.4.pdf](https://datastore.copernicus-climate.eu/documents/satellite-sea-level/D3.SL.1-v1.2_PUGS_of_v1DT2018_SeaLevel_products_v2.4.pdf)
- Mesinger, F., DiMego, G., Kalnay, E., Mitchell, K., Shafran, P. C., Ebisuzaki, W., et al. (2006). North American Regional Reanalysis. *Bulletin of the American Meteorological Society*, 87(3), 343–360. <https://doi.org/10.1175/BAMS-87-3-343>
- Mountain, D. G., & Jessen, P. F. (1987). Bottom waters of the Gulf of Maine, 1978–1983. *Journal of Marine Research*, 45(2), 319–345. <https://doi.org/10.1357/002224087788401160>
- Mountain, D. G., & Manning, J. P. (1994). Seasonal and interannual variability in the properties of the surface waters of the Gulf of Maine. *Continental Shelf Research*, 14(13), 1555–1581. [https://doi.org/10.1016/0278-4343\(94\)90090-6](https://doi.org/10.1016/0278-4343(94)90090-6)
- Mupparapu, P., & Brown, W. S. (2002). Role of convection in winter mixed layer formation in the Gulf of Maine, February 1987. *Journal of Geophysical Research*, 107(C12), 22–1–22–18. <https://doi.org/10.1029/1999JC000116.2218>
- Pershing, A. J., Alexander, M. A., Hernandez, C. M., Kerr, L. A., Le Bris, A., Mills, K. E., et al. (2015). Slow adaptation in the face of rapid warming leads to collapse of the Gulf of Maine cod fishery. *Science*, 350(6262), 809–812. <https://doi.org/10.1126/science.aac9819>
- Petrie, B. (2007). Does the north Atlantic oscillation affect hydrographic properties on the Canadian Atlantic continental shelf? *Atmosphere-Ocean*, 45(3), 141–151. <https://doi.org/10.3137/ao.450302>
- Pettigrew, N. R., Fikes, C. P., & Beard, M. K. (2011). Advances in the Ocean Observing System in the Gulf of Maine: Technical Capabilities and Scientific Results. *Marine Technology Society Journal*, 45(1), 85–97. <https://doi.org/10.4031/MTSJ.45.1.11>
- Ramp, S. R., Schlitz, R. J., & Wright, W. R. (1985). The deep flow through the Northeast Channel, Gulf of Maine. *Journal of Physical Oceanography*, 15, 1790–1808. [https://doi.org/10.1175/1520-0485\(1985\)015<1790:tdfttn>2.0.CO;2](https://doi.org/10.1175/1520-0485(1985)015<1790:tdfttn>2.0.CO;2)
- Rosby, T., & Benway, R. L. (2000). Slow variations in mean path of the Gulf Stream east of Cape Hatteras. *Geophysical Research Letters*, 27(1), 117–120. <https://doi.org/10.1029/1999GL002356>
- Rosby, T., Flagg, C. N., Donohue, K., Sanchez-Franks, A., & Lillibridge, J. (2014). On the long-term stability of Gulf Stream transport based on 20 years of direct measurements. *Geophysical Research Letters*, 41(1), 114–120. <https://doi.org/10.1002/2013GL058636>
- Schlitz, R. J., & Cohen, E. B. (1984). A nitrogen budget for the Gulf of Maine and Georges Bank. *Biological Oceanography*, 3, 203–222.
- Shchepetkin, A. F., & McWilliams, J. C. (2005). The regional oceanic modeling system (ROMS): a split-explicit, free-surface, topography-following-coordinate oceanic model. *Ocean Modelling*, 9(4), 347–404. <https://doi.org/10.1016/j.ocemod.2004.08.002>
- Shchepetkin, A. F., & McWilliams, J. C. (2009). Computational Kernel Algorithms for Fine-Scale, Multiprocess, Longtime Oceanic Simulations. In R. M. Temam, & J. J. Tribbia (Eds.), *Handbook of numerical analysis* (Vol. 14, pp. 121–183). Elsevier. [https://doi.org/10.1016/S1570-8659\(08\)01202-0](https://doi.org/10.1016/S1570-8659(08)01202-0)
- Smith, P. C. (1983). The Mean and Seasonal Circulation off Southwest Nova Scotia. *Journal of Physical Oceanography*, 13(6), 1034–1054. [https://doi.org/10.1175/1520-0485\(1983\)013<1034:TMASCO>2.0.CO;2](https://doi.org/10.1175/1520-0485(1983)013<1034:TMASCO>2.0.CO;2)
- Smith, P. C., Houghton, R. W., Fairbanks, R. G., & Mountain, D. G. (2001). Interannual variability of boundary fluxes and water mass properties in the Gulf of Maine and on Georges Bank: 1993–1997. *Deep Sea Research Part II: Topical Studies in Oceanography*, 48(1), 37–70. [https://doi.org/10.1016/S0967-0645\(00\)00081-3](https://doi.org/10.1016/S0967-0645(00)00081-3)
- Smith, P. C., & Pettigrew, N. R. (2012). Regime Shift in the Gulf of Maine. *American Fisheries Society Symposium*, 79, 185–203.
- Taylor, A. H., & Stephens, J. A. (1998). The North Atlantic oscillation and the latitude of the Gulf Stream. *Tellus A: Dynamic Meteorology and Oceanography*, 50(1), 134–142. <https://doi.org/10.3402/tellusa.v50i1.14517>
- Townsend, D. W. (1998). Sources and cycling of nitrogen in the Gulf of Maine. *Journal of Marine Systems*, 16(3–4), 283–295. [https://doi.org/10.1016/S0924-7963\(97\)00024-9](https://doi.org/10.1016/S0924-7963(97)00024-9)
- Townsend, D. W., Pettigrew, N. R., Thomas, M. A., Neary, M. G., McGillicuddy, D. J., & O'Donnell, J. (2015). Water masses and nutrient sources to the Gulf of Maine. *Journal of Marine Research*, 73(3), 93–122. <https://doi.org/10.1357/002224015815848811>

- Townsend, D. W., Rebeck, N. D., Thomas, M. A., Karp-Boss, L., & Gettings, R. M. (2010). A changing nutrient regime in the Gulf of Maine. *Continental Shelf Research*, 30(7), 820–832. <https://doi.org/10.1016/j.csr.2010.01.019>
- Xue, H., Chai, F., & Pettigrew, N. R. (2000). A Model Study of the Seasonal Circulation in the Gulf of Maine. *Journal of Physical Oceanography*, 30, 1111–1135. [https://doi.org/10.1175/1520-0485\(2000\)030<1111:amsots>2.0.co;2](https://doi.org/10.1175/1520-0485(2000)030<1111:amsots>2.0.co;2)
- Zhang, W., & Lentz, S. J. (2017). Wind-Driven Circulation in a Shelf Valley. Part I: Mechanism of the Asymmetrical Response to Along-Shelf Winds in Opposite Directions. *Journal of Physical Oceanography*, 47(12), 2927–2947. <https://doi.org/10.1175/JPO-D-17-0083.1>
- Zhang, W. G., & Gawarkiewicz, G. G. (2015). Length scale of the finite-amplitude meanders of Shelfbreak Fronts. *Journal of Physical Oceanography*, 45(10), 2598–2620. <https://doi.org/10.1175/JPO-D-14-0249.1>
- Zhang, W. G., Gawarkiewicz, G. G., McGillicuddy, D. J., & Wilkin, J. L. (2011). Climatological Mean Circulation at the New England Shelf Break. *Journal of Physical Oceanography*, 41(10), 1874–1893. <https://doi.org/10.1175/2011JPO4604.1>
- Zhang, W. G., & Partida, J. (2018). Frontal Subduction of the Mid-Atlantic Bight Shelf Water at the Onshore Edge of a Warm-Core Ring. *Journal of Geophysical Research: Oceans*, 123(11), 7795–7818. <https://doi.org/10.1029/2018JC013794>